A portable and dual-inducible control system for multistep biosynthetic pathways in Gram-negative bacteria

Andrés Felipe Carrillo Rincón[1,2], Alexandra J. Cabral[1], Andras Gyorgy[2], Natalie G. Farny[1,3]*

1. Department of Biology and Biotechnology, Worcester Polytechnic Institute, Worcester, MA, USA
2. Division of Engineering, NYU Abu Dhabi, Abu Dhabi, UAE
3. Program in Bioinformatics and Computational Biology, Worcester Polytechnic Institute, Worcester, MA, USA

*Correspondence: nfarny@wpi.edu

Keywords: inducible promoters, dual expression, reporter system, lycopene, β-carotene, luciferase, *Escherichia coli*, *Pseudomonas putida*, *Vibrio natriegens*

Abstract

The successful production of industrially relevant natural products hinges on two key factors: the cultivation of robust microbial chassis capable of synthesizing the desired compounds, and the availability of reliable genetic tools for expressing target genes. The development of versatile and portable genetic tools offers a streamlined pathway to efficiently produce a variety of compounds in well-established chassis organisms. The σ^{70}*lac* and *tet* expression systems have shown effective regulation and robust expression of recombinant proteins across various Gram-negative bacteria. To leverage their advantages, here both expression systems were combined into a single plasmid and assessed for their performance in producing fluorescent reporters as well as the terpenoids lycopene and β-carotene. This rapid approach enabled the straightforward transformation of the well-established microorganisms *Escherichia coli*, *Pseudomonas putida*, and *Vibrio natriegens* into efficient microbial cell factories. The dynamic range and the basal expression levels of the σ^{70} expression systems were further enhanced through the incorporation of translational control mechanisms via toehold switches. This improvement was assessed using the highly sensitive luciferase reporter system. This study presents the development and remaining challenges of a versatile genetic tool that is portable across well-established bacterial chassis and capable of controlling the expression of multiple genes, thus facilitating the biosynthesis and study of natural products.

29 **Graphical Abstract**

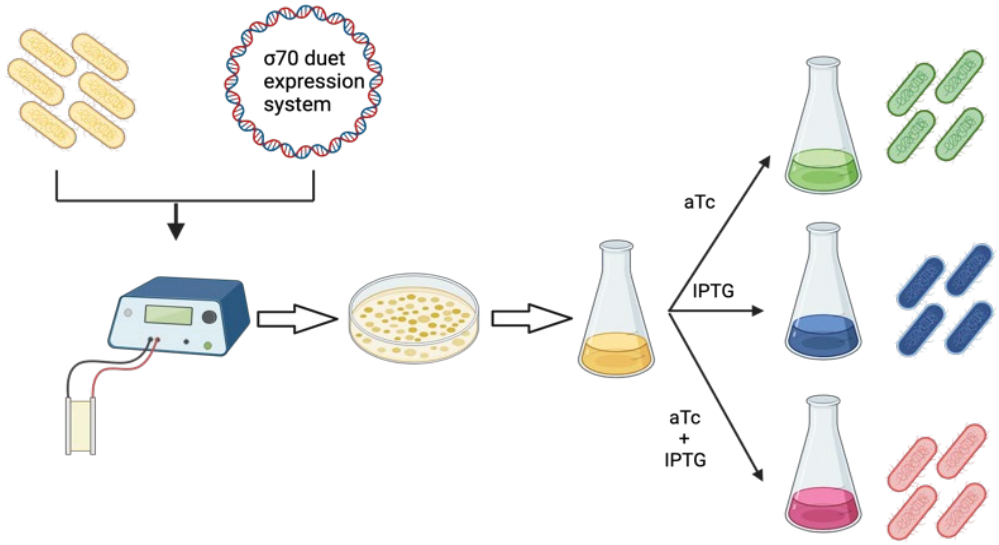

30

31 **Highlights**

32 - A dual-inducible duet-expression system is described for Gram-negative organisms.
33 - Production of lycopene and β-carotene is demonstrated in *E. coli, P. putida,* and *V. natriegens*.
34 - Incorporation of a toehold switch effectively reduces leaky expression of target genes in the
35 uninduced state.
36 - The σ^{70} duet *lac/tet* expression system is a versatile tool for multi-gene biosynthesis across
37 different bacterial chassis.

38

39

40

41 **1. Introduction**

42 Modern sequencing techniques have unveiled a myriad of unknown compounds and proteins
43 encoded by microorganisms with potential industrial applications ranging from biotherapeutics to
44 sustainable manufacturing (Gomez-Escribano, Alt et al. 2016, Wu, Yin et al. 2022). However, these
45 microorganisms are not always easy to cultivate, and manipulating their genes poses a central challenge
46 in unlocking their full potential (Katz and Baltz 2016). *Escherichia coli* is typically the primary choice for
47 expressing proteins from other organisms due to its robust genetic toolkit and well-established cultivation
48 parameters (Baeshen, Al-Hejin et al. 2015). Unfortunately, *E. coli* may struggle to produce toxic genes or
49 complex proteins necessary for the synthesis of natural products (Snijder and Hakulinen 2016, İncir and
50 Kaplan 2024). To overcome these limitations of *E. coli*, alternative hosts like *Pseudomonas putida* and
51 *Vibrio natriegens* have become appealing chassis for producing recombinant proteins. They offer standard
52 laboratory techniques akin to *E. coli*, along with robust genetic and metabolic backgrounds, and rapid
53 growth characteristics (Loeschcke and Thies 2015, Becker, Wimberger et al. 2019). These microorganisms
54 have successfully produced natural products such as non-ribosomal peptides, polyketides, terpenoids,
55 fatty acids, and polymers (Gemperlein, Zipf et al. 2016, Gemperlein, Hoffmann et al. 2017, Ellis, Tschirhart
56 et al. 2019, Hernandez-Arranz, Perez-Gil et al. 2019, Wang, Tschirhart et al. 2020). However, their genetic
57 toolkit is not as versatile and developed as that of *E. coli*.

58 The inducible *tet* and *lac* promoters, optimized for σ^{70} recognition, have shown precise regulation
59 and robust gene overexpression in various Gram-negative bacteria. However, these genetic tools have
60 only been assessed for their efficacy in producing the reporter protein mCardinal and the cocaine esterase
61 CocE (Carrillo Rincón and Farny 2023). Multiple biological processes necessitate the coordinated activity
62 of numerous genes, such as those involved in synthesizing natural products encoded by biosynthetic gene
63 clusters (Jensen 2016, Meyer, Segall-Shapiro et al. 2019). To facilitate multi-gene expression, the pET
64 system was modified to concurrently express various genes within the same *E. coli* BL21 strain using the

65 pETDuet system (Tolia and Joshua-Tor 2006). However, in pETDuet, both multiple cloning sites are induced
66 by IPTG, preventing independent or sequential control (Zhang, Liu et al. 2012). To overcome this
67 limitation, the *E. coli* "marionette" strain was developed containing twelve inducible systems, including
68 the well-known lactose, tetracycline and arabinose expression systems among others (Meyer, Segall-
69 Shapiro et al. 2019). Additionally, the synergistic effect of combined promoters to produce target
70 recombinant proteins in *E. coli* has demonstrated differing levels of success thus far (Öztürk, Ergün et al.
71 2017). A dual-inducible duet expression system was also engineered in *P. putida* utilizing the original *lac*,
72 *tet* and *bad* promoters, resulting in the successful production of fluorescent proteins and an inducible
73 CRISPR interference system (Gauttam, Mukhopadhyay et al. 2020, Gauttam, Mukhopadhyay et al. 2021).
74 Despite these significant achievements, the original promoters utilized in these studies lack the strength
75 and versatility of the optimized σ^{70} *lac* and *tet* promoter (Carrillo Rincón and Farny 2023).

76 Adapting the consensus sequences recognized by the σ^{70} factor to the *lac* and *tet* promoters
77 significantly enhanced their strength, surpassing the efficiency of the pET system in *E. coli* (Carrillo Rincón
78 and Farny 2023). Nevertheless, the uninduced state of the optimal σ^{70}V2LacI expression system was
79 scarcely repressed by its transcriptional regulator LacI, thereby negating the advantages of having an
80 inducible system (Carrillo Rincón and Farny 2023). One strategy to enhance the fold-change and minimize
81 the leaky expression of the target gene, thereby reducing unnecessary consumption of cellular resources
82 required for cell growth, involves the adaptation of toehold switch riboregulators (Hwang, Kim et al.
83 2021). In the toehold-mediated strand displacement (TMSD) strategy, the toehold sequesters the
84 ribosome binding site (RBS) of an mRNA molecule, and translation is activated in the presence of the
85 trigger RNA complementary to the toehold sequence (Wang and Simmel 2022). Toehold switches have
86 shown to significantly enhance the mean dynamic range by over 400-fold (Green, Silver et al. 2014). Thus,
87 incorporating them into strong inducible promoters, like the σ^{70}V2LacI, could effectively reduce leakage
88 in the uninduced state.

In this study, we showed that the strong inducible promoters σ^{70}V2Tc and σ^{70}V2/3Lac, recognized by the σ^{70}, can be tailored for a dual-inducible duet-expression system, facilitating the overexpression of multiple genes in well-studied microorganisms such as *E. coli*, *P. putida*, and *V. natriegens*. The efficacy of this duet expression system was confirmed through the expression of reporter systems mCardinal and sfGFP, as well as the production of terpenoids lycopene and β-carotene. Furthermore, we enhanced the fold-change and minimized the leakiness of these expression systems by incorporating toehold switches, a refinement validated by the sensitive reporter system luciferase. In summary, our findings illustrate that the σ^{70} duet *lac/tet* expression system offers a versatile gene tool for activating multiple genes with various inducers across different bacterial chassis. This approach simplifies the production of multiple recombinant proteins or natural products. Additionally, the incorporation of a toehold switch effectively reduces the expression of target genes in the uninduced state, a crucial feature for sensitive or toxic applications.

101 ## 2. Materials and Methods

102 ### 2. 1 Bacterial strains and culture conditions

103 *E. coli* DH10B, *P. putida* JE90 (Elmore, Furches et al. 2017) and *V. natriegens* V. max (Becker,
104 Wimberger et al. 2019) were cultured in LB media supplemented with Kanamycin when required (50
105 µg/mL for *E. coli* and *P. putida*, and 400 µg/mL for *V. natriegens*). *E. coli* and *P. putida* cells were
106 transformed by electroporation, and *V. natriegens* by chemical transformation with the plasmids listed in
107 Table 1. *E. coli* was cultivated at 37ºC and *P. putida* and *V. natriegens* at 30ºC at 220 rpm.

108 ### 2.2 Plasmid construction

109 Phusion® High Fidelity Polymerase (Thermo Scientific) and primers synthesized by Integrated DNA
110 Technologies (IDT) were used in all PCR amplifications for plasmid construction. Plasmids were
111 constructed using Gibson Assembly EX Cloning Kit or T4 DNA ligase (Thermo Scientific) according to
112 manufacturer's instructions. Plasmids were transformed into ElectroMAX DH10B Cells (Thermo Scientific)
113 according to manufacturer's instructions. Transformants were selected on LB (Miller) agar plates
114 containing 50 mg/L kanamycin sulfate for selection and incubated at 37°C. Plasmids were constructed
115 using a combination of ligation of phosphorylated oligonucleotides, and Gibson Assembly. Sequences of
116 all plasmids were confirmed using Sanger sequencing performed by Quintarabio. The backbone of the
117 pJH0204 vector was modified via Gibson to incorporate in the multicloning site the restriction sites BamHI,
118 NdeI, HindIII, KpnI, EcoRI, PstI, XbaI, NcoI, XhoI and eliminate the EcoRI and NcoI sites from the kanamycin
119 cassette, thus generating the plasmid pJH0204F. Then, the σ^{70}V2TcR-mCardinal transcriptional unit was
120 cloned into pJH0204F using BamHI and PstI. The new plasmid was digested with PstI and XbaI to
121 accommodate the transcriptional unit placI-lacI amplified by PCR flanked by PstI and XbaI. Next, the
122 plasmid was digested with NcoI and XhoI to accommodate mCardinal previously amplified and flanked
123 with the same enzymes. Finally, the plasmid was opened with XbaI and NcoI and the V2Lac and V3Lac

124 promoters were cloned via Gibson generating the plasmid pσ^{70}V2TcR-mCardinal/V2LacI-mCardinal and
125 pσ^{70}V2TcR-mCardinal/V3LacI-mCardinal (Fig. 1). Next the sfGFP was cloned after the σ^{70}V2Tc via NdeI and
126 HindIII generating the plasmids pσ^{70}V2TcR-sfGFP/V2LacI-mCardinal and pσ^{70}V2TcR-sfGFP/V3LacI-
127 mCardinal. The crtEBI genes were PCR amplified adjusting an NdeI at the 5' of crtE and a HindIII at the 3'
128 of the crtI and assembled in the pUC19 vector digested with BamHI and HindIII generating the plasmid
129 pUC19-crtEBI. The crtEBI gene cluster was cloned into pσ^{70}V2TcR via NdeI and HindIII producing the
130 plasmid pσ^{70} V2TcR-crtEBI. Further, crtY was cloned via Gibson into pσ^{70}V2TcR-crtEBI digested with HindIII
131 generating the plasmid pσ^{70}V2TcR-crtEBIY. Finally, the crtY gene was PCR amplified flanked by NcoI and
132 XhoI and cloned to generate the plasmids pσ^{70}V2TcR-crtEBI/V2LacI-crtY and pσ^{70}V2TcR-crtEBI/V3LacI-
133 crtY. The DNA parts containing the σ^{70}V2Tc-THS-trigger/V2Tc-THS-target and σ^{70}V3Lac-THS-trigger/
134 V2Lac-THS-target were synthesized as gBlocks and incorporated via Gibson assembly into the plasmids
135 pJH0204-V2TcR-mCardinal and pJH0204- σ^{70}V3LacI-mCardinal previously digested with BamHI/NdeI and
136 NdeI, respectively. Further, the pσ^{70}V2TcR-Toehold-mCardinal and σ^{70}V3-2LacI-Toehold-mCardinal
137 plasmids were digested with NdeI/HindIII to replace the mCardinal with the luxCDABE operon, previously
138 PCR amplified with appropriate overlapping tails and incorporated into the plasmid via Gibson assembly.
139 To produce the pSC101 plasmids the ampicillin cassette was replaced via Golden Gate assembly. Briefly,
140 the pSC101 was PCR amplified in the outward direction with respect to the ampicillin cassette, creating
141 the backbone amplicon, flanked with BsaI cut sites. The kanamycin cassette was PCR amplified flanked
142 with BsaI cut sites that generate complementary sticky ends to the pSC101 backbone. Both DNA fragments
143 were assembled using the standard Golden Gate protocol generating pSC101-Kn. The cassettes containing
144 the luxCDABE operon with the different expression systems were digested with BamHI and XhoI and
145 cloned into pSC101-Kn previously amplified with primers that incorporated the BamhI/XhoI restriction
146 sites. The complete list of plasmids used and generated in this study is presented in Table 1. Primers

147 (Supplementary Table S1) and DNA sequences used in this study are presented in the supplementary
148 information.

149 **2.3 Measurement of the reporter systems in the plate reader**

150 Growth curves and fluorescence measurements were performed in 96-well clear bottom
151 microplates (Corning Incorporated, NY) using the BioTek Synergy H1 Hybrid Multi-Mode Reader following
152 the experimental approach described in (Krishnamurthi, Niyonshuti et al. 2021). Briefly, overnight cultures
153 of the recombinant strains were diluted into fresh LB medium supplemented with kanamycin to reach
154 OD_{600} 0.05. *E. coli* experiments were performed at 37°C, and *P. putida* and *V. natriegens* at 30°C, shaking
155 at 355 cycles per minute (cpm). Cell density (OD_{600}) and fluorescence (sfGFP excitation 485nm, emission
156 510nm; mCardinal excitation 604nm, emission 659nm) were monitored every hour for 16 hours. *E. coli*
157 cultures were induced at 3 hours with 0.2 mM IPTG and/or 0.1 µg/mL aTc, *P. putida* at 3 hours with 5 mM
158 IPTG and/or 1 µg/mL aTc, and *V. natriegens* at 2 hours with 0.2 mM IPTG and/or 0.1 µg/mL aTc when
159 required.

160 **2.4 Lycopene and β-carotene determination**

161 Lycopene and β-carotene were measured by UHPLC following the procedure described in
162 (Bohoyo-Gil, Dominguez-Valhondo et al. 2012) using a Shimadzu Nexera UHPLC. Lycopene and β-carotene
163 were extracted with acetone as described in (Xu, Xu et al. 2018) with the following modifications. 5% of
164 overnight cultures of the recombinant *E. coli*, *P. putida* and *V. natriegens* strains containing either the LYC
165 operon or the crtEBIY genes were inoculated in 5 mL of fresh LB media supplemented with kanamycin and
166 grown at 220 rpm and 37°C for *E. coli* and 30°C for *P. putida* and *V. natriegens*. The cultures were induced
167 at OD_{600} 0.7 with aTc, IPTG, or both accordingly. After the induction the cultures were grown for 4 hours,
168 2 mL samples were collected, centrifuged at 14,000 rpm, the supernatant was discarded, and the cell
169 pellets were stored at -80°C. The cell pellets were resuspended with 200 µL acetone and incubated at 55°C

170 for 15 min in the dark followed by centrifugation at 14,000 rpm, then the supernatant was filtered through
171 a 0.22 µm pore-size nylon membrane for UHPLC analysis. Peak values at 460nm were measured for
172 analysis. Standard curves were generated and used to calculate concentration, shown in Supplementary
173 Figures S1 and S2.

174 Bacterial cultures for UV-vis spectrophotometric analysis were backdiluted to OD600 = 0.05,
175 grown at 30°C or 37°C as appropriate for the strain, then induced with aTc at three hours, then grown for
176 an additional 17 hours. Carotenoids were extracted for UV-vis spectrophotometric analysis by acetone
177 extraction as described (Alper, Miyaoku et al. 2005). Briefly, 5mL of each culture was spun down, media
178 was discarded from the bacterial pellet, and the pellet was re-suspended in 2.5mL of acetone. Samples
179 were heated at 55ºC for 15 minutes with intermittent vortexing. Samples were spun and the lycopene or
180 β-carotene content in the supernatant was analyzed by UV-vis spectrophotometry. The determination of
181 carotenoid concentration by UV-vis spectrophotometry was performed by scanning from 300 – 600nm on
182 a Thermo Scientific Evolution 300 Spectrophotometer, essentially as described (Karnjanawipagul,
183 Nittayanuntawech et al. 2010), using measurements at 456nm for β-carotene and 474nm for lycopene.
184 Standard curves were generated and used to calculate concentration, shown in Supplementary Figures S3
185 and S4.

186 **2.5 Bioluminescence assay**

187 *E. coli* or *P. putida* overnight cultures supplemented with kanamycin (LB, 37°C with shaking, 220 rpm)
188 were diluted 1/200 in fresh LB in 96-well clear bottom microplates (Corning Incorporated, NY) shaking at
189 355 cycles per minute (cpm) and induced after three hours of growth with 0.2/ 5 mM IPTG and 0.1/1.0
190 µg/mL aTc accordingly. Bioluminescence (gain: 100) and cell density (OD_{600}) were monitored every 20
191 minutes with the BioTek Synergy H1 Hybrid Multi-Mode Reader instrument for 20 hours.

192

193 **3. Results and Discussion**

194 **3.1 Development of the dual expression system**

195 The σ^{70}V2TcR and σ^{70}V3LacI expression systems exhibited tight regulation and robust induction in
196 *E. coli* in the presence of anhydrotetracycline (aTc) and IPTG, respectively, while in *P. putida* and *V.*
197 *natriegens* the σ^{70}V2TcR and σ^{70}V2LacI demonstrated superior performance as inducible promoters
198 (Carrillo Rincón and Farny 2023). Our previous findings indicated that multicopy plasmids like pUC19
199 cannot effectively support LacI expression, even with its native weak promoter. Therefore, we developed
200 the dual expression system using the pJH0204 vector as a backbone, which contains the pColE1 replication
201 origin and *attB* sites specific for the bxb1 recombinase (Elmore, Dexter et al. 2023). Each transcriptional
202 unit of the dual expression system was insulated by terminators (Kelly, Taylor et al. 2019), and the
203 transcriptional regulators *tetR* and *lacI* were positioned between and in opposite directions of the
204 inducible promoters σ^{70}V2Tc and σ^{70}V2Lac or σ^{70}V3Lac (σ^{70}V2/3Lac), blocking undesired transcription of
205 the open reading frames (ORF). Additionally, two different multiple cloning sites were placed after the
206 inducible promoters σ^{70}V2Tc and σ^{70}V2/3Lac to facilitate the incorporation of target genes (Fig. 1A).

207 The dual expression system was assessed in *E. coli*, *P. putida*, and *V. natriegens* to evaluate: i)
208 independent control of two different fluorescent proteins, ii) potential synergy when expressing the same
209 protein, and iii) control of the biosynthetic gene cluster (BGC) responsible for the biosynthesis of lycopene
210 and β-carotene. Expression of various recombinant proteins was achieved by placing sfGFP under the
211 control of σ^{70}V2TcR and mCardinal under the control of σ^{70}V2/3LacI (Fig. 1C). Synergy was gauged using
212 the reporter system mCardinal, which was incorporated into both inducible promoters of the dual
213 expression system (Fig. 1B). Finally, production of the terpenoids lycopene and β-carotene by the dual
214 expression system was achieved by the assembly of the crtEBIY genes from *Pantoea ananatis* (Hernandez-
215 Arranz, Perez-Gil et al. 2019), which were synthesized with the codon usage for *E. coli.* The crtEBI (LYC

216 operon) was assembled in the pUC19 vector via Gibson assembly, adapting the ribosome binding site
217 (RBS) of J23119 (Gong, Liu et al. 2016) to crtB and the RBS pJL1 (Wang, Li et al. 2018) to crtI, then the
218 synthetic construct was transferred to the σ^{70}V2TcR expression system to evaluate lycopene production
219 (Fig. 1D). β-carotene production was evaluated with the incorporation of the crtY gene with the J23119
220 RBS to σ^{70}V2TcR-crtEBI yielding σ^{70}V2TcR-crtEBIY (Fig. 1E). The dual control of the crtEBI operon together
221 with the crtY gene to produce β-carotene was achieved by adapting the crtEBI to the σ^{70}V2TcR expression
222 system and the crtY gene to σ^{70}V2/3LacI expression system present in the dual vector (Fig. 1F).

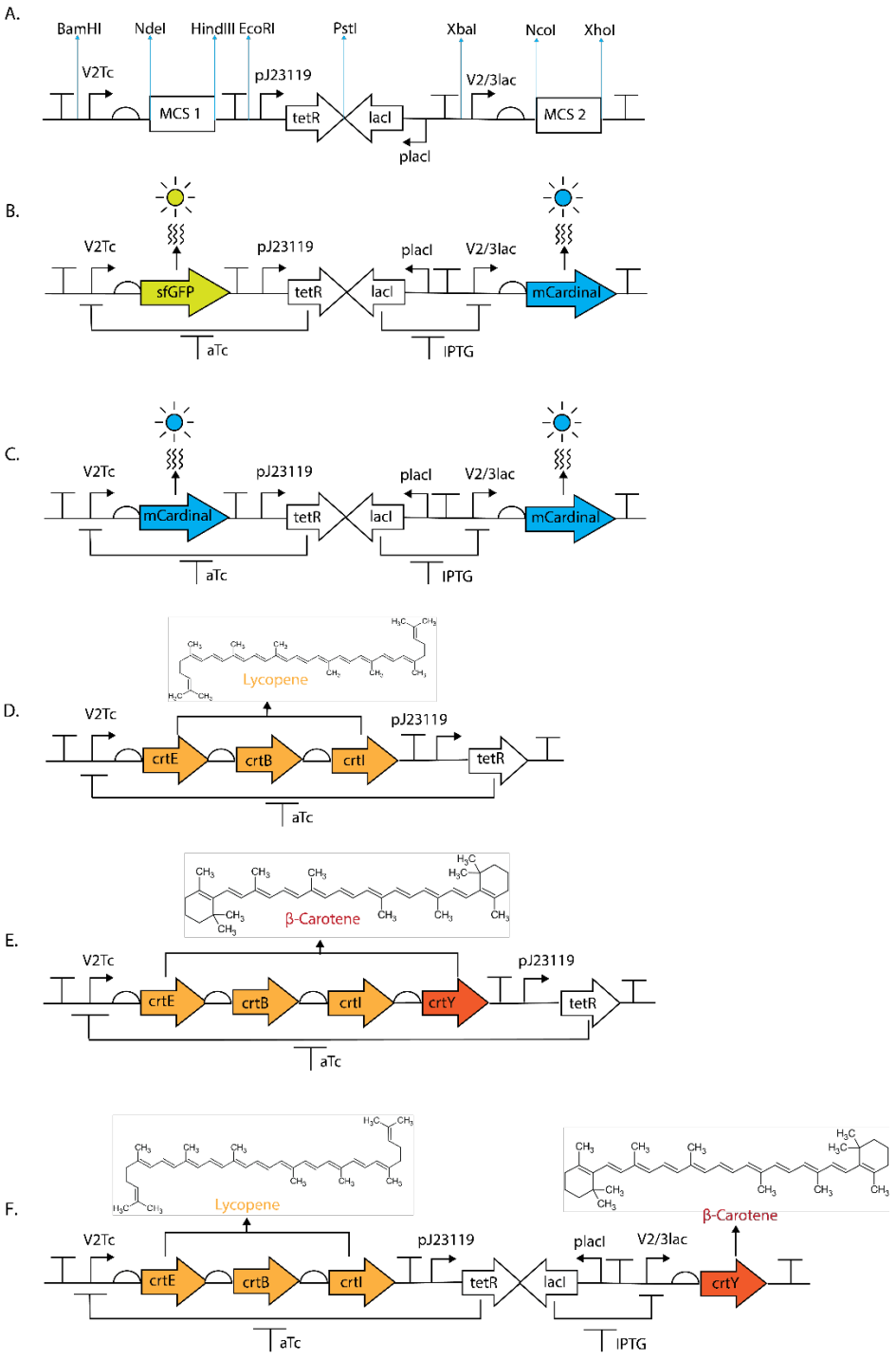

Figure 1. Genetic circuits used in this study. A. Design of the dual expression systems σ^{70}V2TcR-V2LacI and σ^{70}V2TcR-V3LacI. **B.** Dual expression system controlling expression of sfGFP from the σ^{70}V2Tc promoter and mCardinal from the σ^{70}V2Lac or σ^{70}V3Lac promoters. The σ^{70}V3Lac promoter constructs are used for expression in *E. coli*, and the σ^{70}V2Lac constructs are used in *P. putida* and *V. natriegens.* **C.** Dual expression system controlling expression of mCardinal under both the σ^{70}V2Tc promoter and the σ^{70}V2Lac or σ^{70}V3Lac promoter. **D.** σ^{70}V2TcR expression system controlling the LYC operon (crtEBI) for lycopene production. **E.** σ^{70}V2TcR expression system controlling expression of crtEBIY for β-carotene production. **F.** Dual expression system controlling expression of crtEBI from the σ^{70}V2Tc promoter and crtY from the σ^{70}V2LacI or σ^{70}V3LacI promoters.

231 **Table 1.** List of plasmids evaluated in this study.

Name	Expression system 1	ORF1	Expression system 2	ORF2	Source
pσ^{70} V2TcR-mCardinal	V2TcR	mCardinal			(Carrillo Rincón and Farny 2023)
pσ^{70} V2lacI-mCardinal	V2lacI	mCardinal			(Carrillo Rincón and Farny 2023)
pσ^{70} V3LacI-mCardinal	V3LacI	mCardinal			(Carrillo Rincón and Farny 2023)
pσ^{70} V2TcR-sfGFP	V2TcR	sfGFP			(Carrillo Rincón and Farny 2023)
pσ^{70} V2lacI-sfGFP	V2LacI	sfGFP			(Carrillo Rincón and Farny 2023)
pσ^{70} V3LacI-sfGFP	V3LacI	sfGFP			(Carrillo Rincón and Farny 2023)
pJH0204F					This study
pσ^{70} V2TcR-mCardinal/V2LacI-mCardinal	V2TcR	mCardinal	V2LacI	mCardinal	This study
pσ^{70} V2TcR-mCardinal/V3LacI-mCardinal	V2TcR	mCardinal	V3LacI	mCardinal	This study
pσ^{70} V2TcR- sfGFP/V2LacI-mCardinal	V2TcR	mCardinal	V2LacI	sfGFP	This study
pσ^{70} V2TcR- sfGFP/V3LacI-mCardinal	V2TcR	mCardinal	V3LacI	sfGFP	This study
pUC19-crtEBI	-	crtEBI			This study
pσ^{70} V2TcR-crtEBI	V2TcR	crtEBI			This study
pσ^{70} V2TcR-crtEBIY	V2TcR	crtEBIY			This study
pσ^{70} V2TcR-crtEBI/V2LacI-crtY	V2TcR	crtEBI	V2LacI	crtY	This study
pσ^{70} V2TcR-crtEBI/V3LacI-crtY	V2TcR	crtEBI	V3LacI	crtY	This study
pσ^{70} V2TcR-Toehold-mCardinal	V2TcR	mCardinal			This study

pσ^{70} V3-2LacI-Toehold-mCardinal	V3-2LacI	mCardinal			This study
pσ^{70} V2TcR-Toehold-luxCDABE	V2TcR	luxCDABE			This study
pσ^{70} V3-2LacI-Toehold-luxCDABE	V3-2LacI	luxCDABE			This study
pσ^{70} V2TcR -luxCDABE	V2TcR	luxCDABE			This study
pσ^{70} V2LacI-luxCDABE	V2LacI	luxCDABE			This study
pSC101-Kn					This study
pSC101Kn σ^{70} V2TcR -luxCDABE	V2TcR	luxCDABE			This study
pSC101Kn σ^{70} V2LacI-luxCDABE	V2LacI	luxCDABE			This study
pSC101Kn σ^{70} V2TcR-Toehold-luxCDABE	V2TcR	luxCDABE			This study
pSC101Kn σ^{70} V3-2LacI-Toehold-luxCDABE	V3-2LacI	luxCDABE			This study

232

233

234 **3.2 Independent and concurrent control of two fluorescent proteins with the dual expression system**

235 Duet vectors are available for *E. coli* and *Pseudomonas fluorescens*, but they are solely inducible
236 by either IPTG or arabinose (Tolia and Joshua-Tor 2006, Nakata 2017), whereas dual-inducible duet
237 expression vectors have been developed specifically for *Corynebacterium glutamicum* (Gauttam,
238 Desiderato et al. 2019) and *P. putida* (Gauttam, Mukhopadhyay et al. 2020, Gauttam, Mukhopadhyay et
239 al. 2021). Unfortunately, there is currently no a versatile dual overexpression system that permits the
240 differential expression of distinct sets of genes through two independent inducible promoters, which can
241 be used across various Gram-negative species. We have previously demonstrated the strength and
242 portability of the σ^{70}V2TcR and σ^{70}V2/3LacI promoters separately in *E. coli, P. putida*, and *V. natriegens*
243 (Carrillo Rincón and Farny 2023). Thus, to test the independent and concurrent regulation of two proteins
244 simultaneously from these promoters, we introduced two different reporter proteins into the dual-
245 inducible σ^{70}V2TcR/V2LacI and σ^{70}V2TcR/V3LacI expression systems (Fig. 1B) and assessed their
246 production in *E. coli*, *P. putida*, and *V. natriegens*. Specifically, the transcriptional unit V2TcR controlled
247 the expression of sfGFP, while the V2LacI or V3LacI unit regulated mCardinal production (Fig. 2). This
248 configuration was selected because the species under investigation are susceptible to autofluorescence
249 in the yellow-green spectrum, which could interfere with the measurement of sfGFP (Carrillo Rincón and
250 Farny 2023). The σ^{70}V2TcR promoter was therefore selected to regulate the expression of sfGFP due to its
251 tighter control in the OFF state, facilitating a more sensitive estimation of the production of the reporter
252 system. On the other hand, the σ^{70}V2/3LacI systems, which tend to leak considerably in *V. natriegens*
253 (Carrillo Rincón and Farny 2023), control the expression of the far-red fluorescent protein mCardinal.
254 Importantly, at this wavelength, the cells do not produce endogenous fluorescence (Canty, Hariharan et
255 al. 2018).

256 To create a direct comparison, the induction of the individual expression systems σ^{70}V2TcR-sfGFP
257 and σ^{70}V2/3LacI-mCardinal were measured in *E. coli* (Fig. 2A), *P. putida* (Fig. 2B) and *V. natriegens* (Fig.

258 2C). The dual-inducible σ^{70}V2TcR/V2LacI and σ^{70}V2TcR/V3LacI expression systems were also measured in
259 the same species (Fig. 2D-F). Under the control of σ^{70}V2TcR, sfGFP production was higher in the dual
260 system by 1.2-fold in *E. coli* and *P. putida*, and 1.7-fold in *V. natriegens* at 16 hours of induction (Fig. 2D-
261 F, left panels). However, an opposite trend was observed in the dual expression system for production of
262 mCardinal under the control of σ^{70}V2/3LacI, which was significantly reduced, resulting in 6.2-fold, 2.4-fold,
263 and 2.0-fold less red emission in *E. coli*, *P. putida*, and *V. natriegens*, respectively (Fig. 2D-F, right panels).

264 Interestingly, when the cultures containing the dual expression system were co-induced with aTc
265 and IPTG, both green and red fluorescence reached comparable levels compared to cultures induced with
266 only one inducer. So, while the maximum expression from each promoter was distinct from the maxima
267 achieved in the single promoter systems, concurrent induction of both promoters did not impact their
268 transcriptional output. This suggests that the promoters (σ^{70}V2TcR and σ^{70}V2/3LacI) are barely affected
269 by the activation of the other, reaching almost their maximum activity either upon sole activation or
270 concurrent activation (Fig. 2G). The three bacterial species investigated, each containing the dual
271 expression system, displayed barely detectable green fluorescence in the uninduced state, indicating tight
272 regulation of the σ^{70}V2TcR expression system (Fig. 2G). However, as expected, some mCardinal leakage
273 was observed originating from the σ^{70}V2LacI-mCardinal expression system in *V. natriegens* (Fig. 2F-G).

274 The dual expression system constitutively expresses the transcriptional regulators TetR and LacI,
275 both of which have been reported to exhibit toxicity at high concentrations (Lutz and Bujard 1997,
276 Romanuka, van den Bulke et al. 2009, Stetz, Carter et al. 2016), and each sensor requires cellular resources
277 (for example, ribosomes) to function, and the activation of one sensor can influence another indirectly
278 due to resource competition (Gyorgy, Jiménez et al. 2015). We anticipated a lower performance for both
279 promoters in the dual expression system, due to the metabolic burden imposed by the simultaneous
280 presence of TetR and LacI. However, this scenario was only observed with σ^{70}V2/3LacI, which exhibited
281 reduced production of mCardinal, which was particularly pronounced in *E. coli*, thus suggesting its

282 sensitivity to both transcriptional regulators. Conversely, the levels of sfGFP appeared to be enhanced by
283 σ^{70}V2TcR in the dual expression system. One hypothesis for this observation is that the stress response
284 triggered by the combination of expressing two toxic regulators in the presence of aTc results in the
285 induction of the RpoS regulon, causing increased expression of *rpoB* and several genes involved in
286 nucleotide salvage and purine biosynthesis (Bie, Zhang et al. 2023). Furthermore, it leads to the induction
287 of heat shock proteins (Bie, Zhang et al. 2023). Additionally, there is increased transcription of genes
288 participating in the SOS pathway, promotion of glucose metabolism, and induction of the oxidative stress
289 response (Bie, Zhang et al. 2023). To mitigate the adverse effect of these stresses, the cells produce
290 endogenous fluorophores and/or metabolic byproducts increasing the green emission of green light
291 (Monici 2005). For instance, *P. putida* secretes pyoverdine, a soluble fluorescent yellow-green pigment,
292 under iron-limiting conditions (Ringel and Brüser 2018). We predict that the σ^{70}V2TcR in the dual
293 expression system did not in fact display increased transcriptional activity. Instead, it is possible that the
294 presence of endogenous molecules interfering in the green spectrum, not originating from the
295 recombinant protein, amplified the sfGFP signal due to activation of cellular stress responses.

296

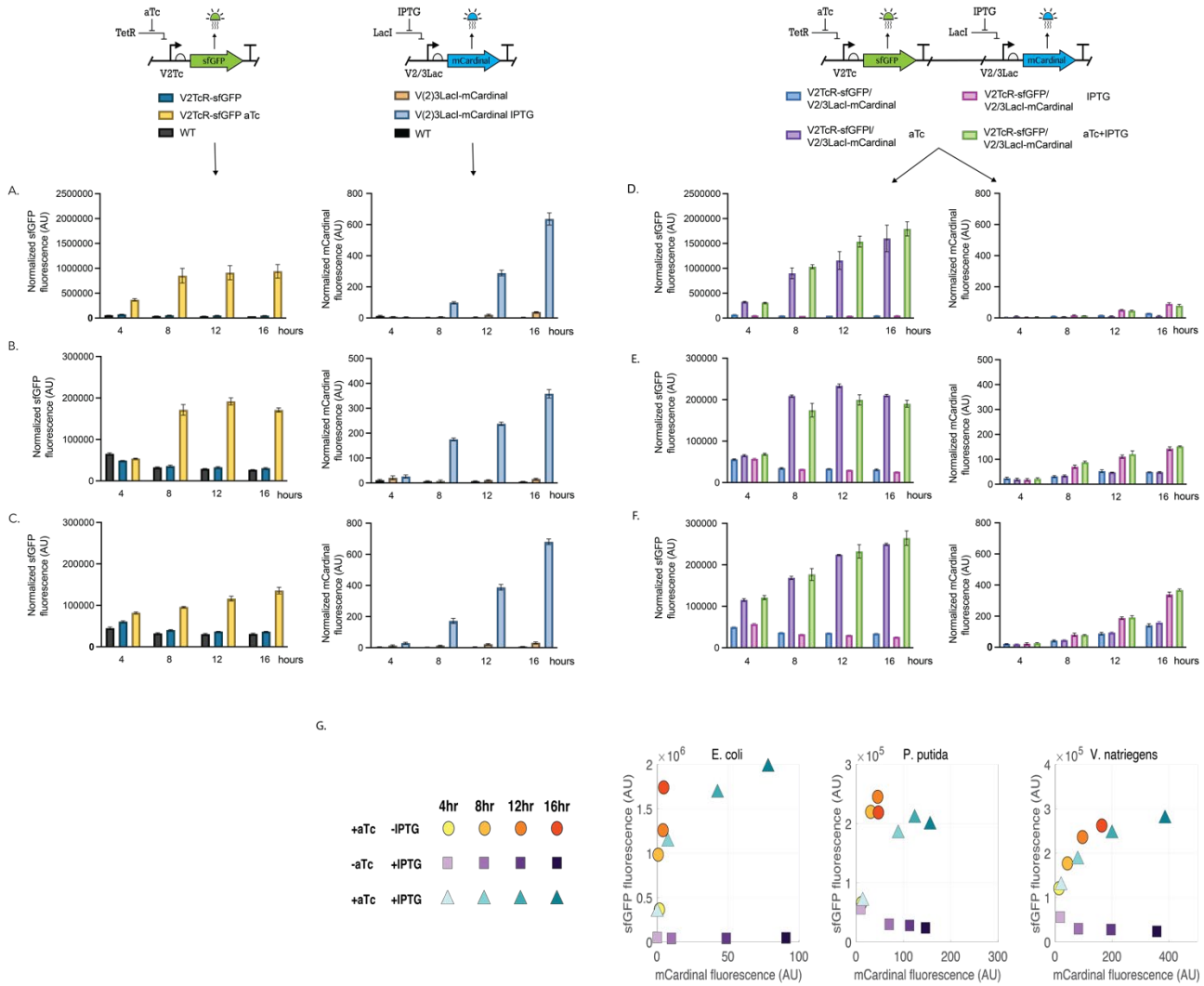

Figure 2. sfGFP and mCardinal production in *E. coli*, *P. putida*, and *V. natriegens* containing the dual expression. For all samples, the fluorescence mean of sfGFP signal (excitation 485, emission 510) and mCardinal signal (excitation 605, emission 659) was normalized by the cell density (OD_{600}). **A-C.** *E. coli* (A), *P. putida* (B) and *V. natriegens* (C) expressing the single reporter systems σ^{70}V2TcR-sfGFP (left panels) or σ^{70}V2/3LacI-mCardinal (right panels). **D-F.** *E. coli* (D), *P. putida* (E) and *V. natriegens* (F) expressing the dual expression systems σ^{70}V2TcR-sfGFP/σ^{70}V3LacI-mCardinal (in *E. coli*) and σ^{70}V2TcR-sfGFP/σ^{70}V2LacI-mCardinal (in *P. putida* and *V. natriegens*) and measuring sfGFP (left panels) and mCardinal (right panels). Error bars are +/- S.D., n=3. **G.** Matrix display of both sfGFP and mCardinal expression of individual and concurrent inductions of the dual expression systems.

3.3 Evaluating synergistic potential and metabolic cost of the dual expression system

From our first dual expression system experiments, we anticipated a metabolic cost to the cell. We observed that while sfGFP fluorescence from the σ^{70}V2Tc promoter increased relative to a single expression system, mCardinal fluorescence from the σ^{70}V2/3Lac promoters was significantly decreased.

310 If, as we hypothesized, the increased sfGFP was an artifact of cellular stress caused by the combination of
311 metabolic load and aTc exposure, then one would predict that driving the same protein from both
312 promoters would have no synergistic effect on expression over a single promoter system. We have
313 previously shown that increasing the copy number of the same promoter type in *E. coli* effectively
314 enhanced the production of mCardinal by the σ^{70}V2TcR expression system, while it had a detrimental
315 effect on the σ^{70}V3LacI expression system due to the toxicity associated with the transcriptional regulator
316 LacI (Carrillo Rincón and Farny 2023). Hence, to test the synergistic potential of the duet expression
317 system σ^{70}V2TcR/V3LacI, a version was made where both promoters regulate mCardinal (Fig 1C). The *E.*
318 *coli* strain harboring the duet expression system σ^{70}V2TcR/V3LacI exhibited 2-fold and 4-fold lower red
319 fluorescence compared (Fig. 3B) to strains containing σ^{70}V2TcR and σ^{70}V3LacI individually when induced
320 with aTc and IPTG, respectively (Fig. 3A). This observation supports the hypothesis that the increased
321 fluorescence signal in the σ^{70}V2TcR/V3LacI was an artifact of some kind, possibly a product of cellular
322 stress. Synergy was observed by the addition of IPTG and aTc to the σ^{70}V2TcR/V3LacI *E. coli* strain
323 improving mCardinal production by 1.5-fold against the induction obtained with aTc alone (Fig. 3B).
324 However, the mCardinal production in the duet system reached about the same total amount of
325 mCardinal as the σ^{70}V2TcR expression system alone (Fig. 3A,B). These results indicate that the tandem
326 version of the synthetic promoters σ^{70}V2TcR/V3LacI does not offer a real synergy in *E. coli*, but rather an
327 alternative to co-express different genes at high levels using different inducers.

328 In *P. putida* the σ^{70}V2TcR expression system exhibited similar performance in the single and dual
329 version (Fig. 3C & D). Conversely, induction of the dual system with IPTG resulted in a 3-fold decrease
330 relative to the σ^{70}V2lacI system alone (Fig. 3C & D). The simultaneous addition of both inducers (aTc and
331 IPTG) increased mCardinal expression by 1.1-fold over the σ^{70}V2TcR and σ^{70}V2LacI expression systems in
332 the dual system, demonstrating a minimal, statistically insignificant synergistic effect in this host. The duet
333 expression system σ^{70}V2TcR/V2LacI markedly reduced the efficiency of the synthetic promoters in *V.*

334 *natriegens* compared to their single expression system counterparts, with reductions of 12-fold and 2-fold
335 for σ^{70}V2LacI and σ^{70}V2TcR after induction with IPTG and aTc, respectively (Fig. 3E,F). Co-induction of the
336 dual expression system with IPTG and aTc did not yield a synergistic effect in mCardinal production, but
337 achieved similar yields as obtained by induction with aTc alone (Fig. 3F).

338 This information collectively demonstrates that synergy cannot be attained with the dual
339 expression system in *E. coli* and *V. natriegens*. In these two microorganisms, the pJH0204 plasmid
340 containing the pColE1 origin of replication was used, rendering 30 copies per cell in *E. coli* and 300 copies
341 per cell in *V. natriegens*. (Hershfield, Boyer et al. 1974, Tschirhart, Shukla et al. 2019). On the contrary,
342 the duet expression system appears to attenuate the activity of each promoter. Rewiring the cell
343 metabolism imposes additional stress which affects protein synthesis and growth rate (Snoeck, Guidi et
344 al. 2024). Consequently, the constitutive expression of the transcriptional regulators TetR and LacI, as well
345 as competition for the σ^{70} factor by both promoters, may pose a significant metabolic burden. This triggers
346 energetic inefficiency within the cell, leading to undesirable physiological changes and placing hidden
347 constraints on host productivity (Wu, Yan et al. 2016). In *P. putida*, the dual expression system was directly
348 integrated into the chromosome, thereby reducing the quantities of the transcriptional regulators TetR
349 and LacI and thus lowering the metabolic cost of the synthetic expression systems. This resulted in similar
350 mCardinal production with σ^{70}V2TcR, while the σ^{70}V2LacI expression system showed reduced strength.

351

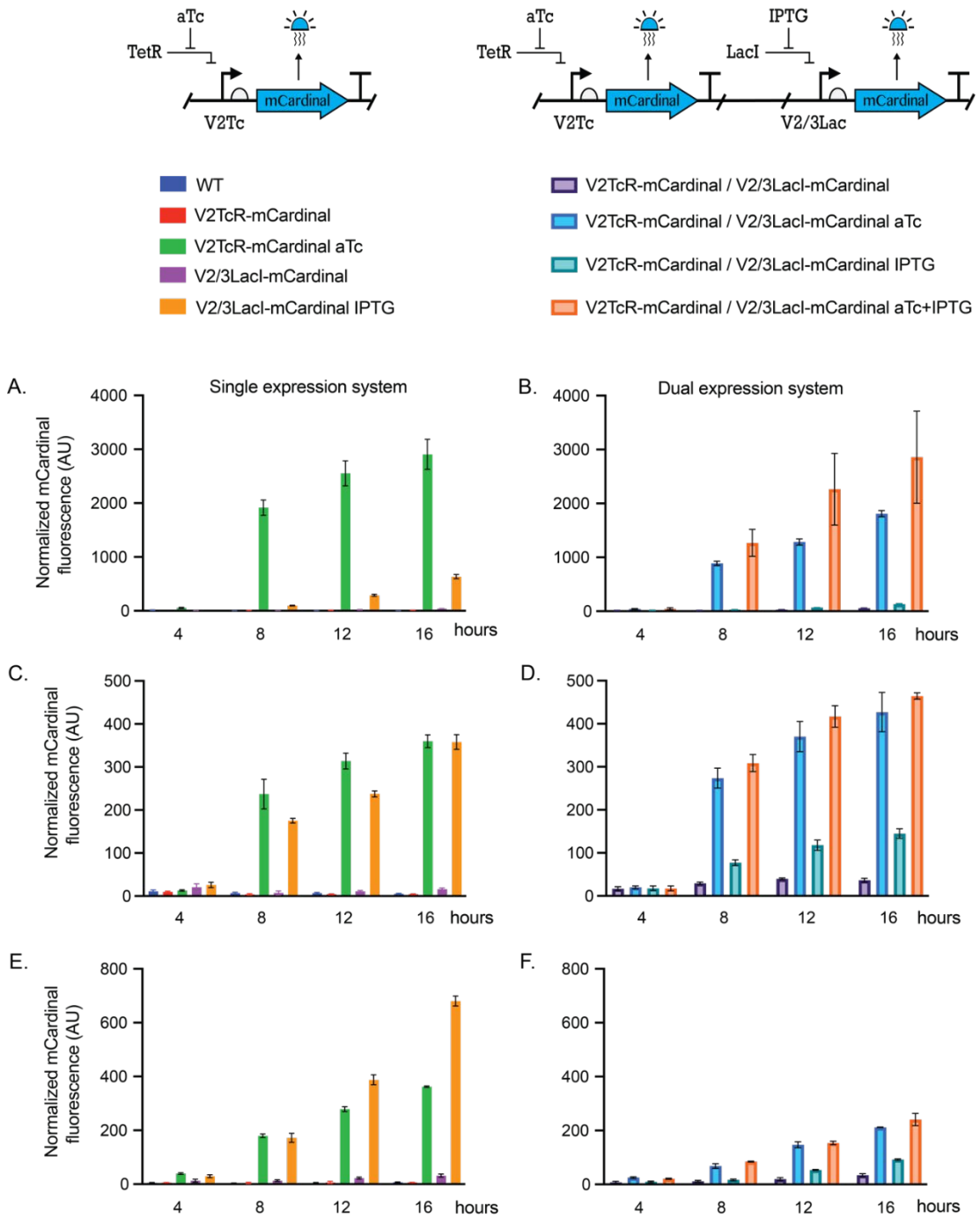

352

353 **Figure 3. Assessing potential synergy between *lac* and *tet* promoters**. (**A, C, E**) Time course of mCardinal production from the
354 single expression systems σ^{70}V2TcR-mCardinal and σ^{70}V3LacI-mCardinal (for *E. coli*) and σ^{70}V2LacI-mCardinal (for *P. putida* and
355 *V. natriegens*) in *E. coli* (**A**), *P. putida* (**C**) and *V. natriegens* (**E**). (**B, D, F**) Single and double inductions of the dual σ^{70}V2TcR-
356 mCardinal/V2LacI-mCardinal or σ^{70}V2TcR-mCardinal/V2LacI-mCardinal expression system in *E. coli* (**B**), *P. putida* (**D**) and *V.*
357 *natriegens* (**F**). For all samples, the fluorescence mean of mCardinal signal (excitation 605nm, emission 659nm) was normalized
358 by the cell density (OD_{600}). Error bars are +/- S.D., n=3.

359 **3.4 Production of lycopene and β-carotene in *E. coli*, *P. putida* and *V. natriegens* using the σ^{70}V2TcR**
360 **single expression system**

361 To assess the capability of the dual expression system to produce natural products, we tested the
362 ability of the σ^{70}V2TcR expression system to control the synthesis of multiple genes in a biosynthetic gene
363 cluster (BGC). To do so, we evaluated the production of lycopene and β-carotene. Lycopene production
364 has already been demonstrated in *E. coli* and *P. putida* through heterologous expression of the lycopene-
365 producing operon (LYC), which contains the crtEBI genes from *Pantoea ananatis* (Hernandez-Arranz,
366 Perez-Gil et al. 2019). Lycopene serves as the biosynthetic precursor of β-carotene. Therefore, the
367 expression of the LYC operon together with crtY leads to β-carotene production. This process has also
368 been demonstrated in *E. coli* and *V. natriegens* (Yoon, Park et al. 2007, Ellis, Tschirhart et al. 2019). The
369 LYC and crtEBIY operons were incorporated into the σ^{70}V2TcR expression system (Fig. 1D,E) and the
370 production of lycopene and β-carotene was quantified using UHPLC (Bohoyo-Gil, Dominguez-Valhondo et
371 al. 2012) after 4 hours of induction with aTc. In *E. coli*, production of both lycopene and β-carotene was
372 achieved. However, the induced culture only yielded 1.7-fold more lycopene and 1.2-fold more β-carotene
373 compared to the uninduced culture when induced for four hours (Fig. 4A, B). Upon a longer induction of
374 17 hours, there was no significant difference in lycopene or β-carotene yields between induced and
375 uninduced cultures (Fig. 4C, D, and Supplementary Figure S5). A decrease in lycopene production was
376 noted with longer induction times under these longer culture conditions (Fig. 4C), which may be due to
377 the documented toxicity of high lycopene production in *E. coli* (Miguez et al., 2018). The results
378 demonstrate that the tight control of the σ^{70}V2TcR system is still unable to completely repress the
379 expression of the crtEBI and crtEBIY BGCs in *E. coli*. A similar observation has been previously published,
380 where lycopene biosynthesis in *E. coli* was controlled using the pET expression system, and also showed
381 significant leakage, with production reaching only 1.1-fold more after 40 hours of induction than the
382 uninduced culture (Xu, Xu et al. 2018). Clearly, the tight regulation of terpenoid biosynthesis in *E. coli*
383 remains a significant challenge.

384 The σ^{70}V2TcR expression system produced a maximum 0.8 mg/L of lycopene in *E. coli* cultivated
385 in a culture tube after only 7 hours of growth (4 hours with the inducer aTc) (Fig. 4A), and a maximum of
386 0.46 mg/L β-carotene after 20 hours of growth (17 hours with the inducer aTc) (Fig. 4D). Notably, no media
387 optimizations were performed, nor any strain engineering beyond the addition of the crtEBI or crtEBIY
388 BGCs. While higher yields have been reported in *E. coli* in different strains, larger bioreactors, and
389 optimized media conditions (Xu, Xu et al. 2018), our results suggest that the σ^{70}V2TcR expression system
390 may contribute yet a further point of optimization to this system by increasing the strength and control
391 of the BGCs.

392 In recombinant strains of *P. putida* and *V. natriegens* containing the σ^{70}V2TcR-crtEBI and
393 σ^{70}V2TcR-crtEBIY transcriptional units, little to no lycopene or β-carotene production was detected
394 without induction. In both organisms, induction of the BGC by aTc led to the robust production of the
395 terpenoids (Fig. 4A-D). *P. putida* was reported to produce 0.0012 µg/L of lycopene after 24 hours of
396 growth with the pSEVA421 vector (Hernandez-Arranz, Perez-Gil et al. 2019). With the σ^{70}V2TcR expression
397 system, lycopene production reached 170 µg/L after only 4 hours of induction (Fig. 4A), and 1028 µg/L
398 after 17 hours of induction (Fig. 4C), marking a substantial increase in reported yield. Additionally, β-
399 carotene production by *P. putida* reached 761 µg/L, the highest yield among the three species in our study
400 (Fig. 4D). *V. natriegens* was reported to produce 500 µg/L of β-carotene cultivated in the rich medium
401 LBv2 for 20 hours (Ellis, Tschirhart et al. 2019), while in the σ^{70}V2TcR expression system achieved 286 µg/L
402 of lycopene (Fig. 4A) and 353 µg/L of β-carotene (Fig. 4B) in the standard LB medium and four hours of
403 induction with no particular optimization. These yields confirm the advantages of the σ^{70}V2TcR expression
404 system, and suggest that significantly increased yields would be possible in the future with the
405 combination of our expression system and other optimizations. The overall results demonstrate that the
406 σ^{70}V2TcR expression system can be efficiently used to drive production of BGCs across a range of Gram-
407 negative bacteria.

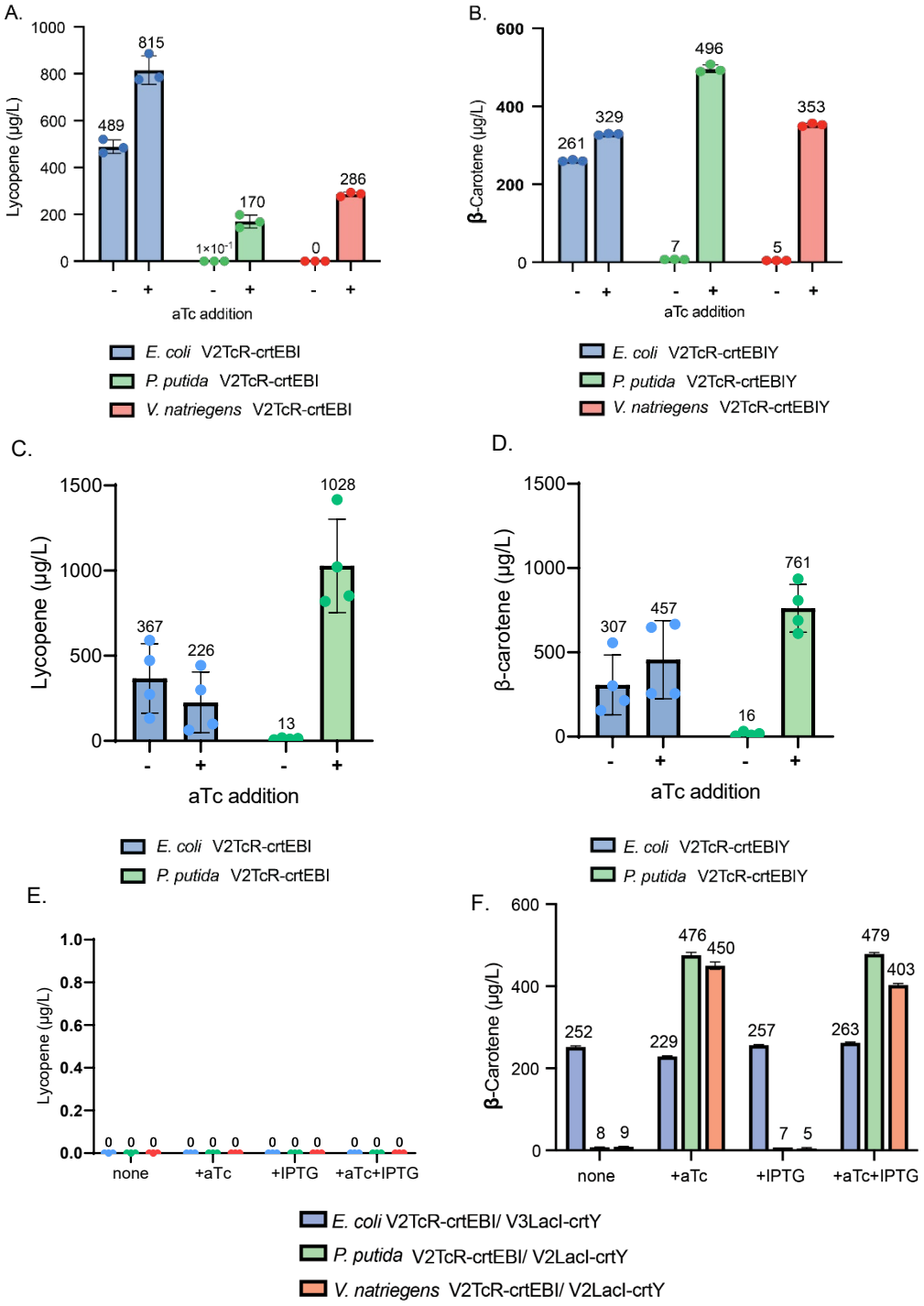

Figure 4. Production of lycopene and β-carotene with the σ^{70}V2TcR expression system in *E. coli, P. putida,* and *V. natriegens*. Production of lycopene (**A**) and β-carotene (**B**) by the single σ^{70}V2TcR expression system expression system in E. *coli, P. putida* and *V. natriegens* was measured by UHPLC by induction of OD_{600}= 0.7 cultures with aTc for 4 hours. Production of lycopene (**C**) and β-carotene (**D**) by the single σ^{70}V2TcR expression system expression system in E. *coli* and *P. putida* was measured by UV-vis spectrophotometry by induction of OD_{600}= 0.05 cultures with aTc for 17 hours. Production of lycopene (**E**) and β-carotene (**F**) by the dual expression system in *E. coli, P. putida* and *V. natriegens*. Cultures were induced with aTc, IPTG or both inducers at OD_{600}.= 0.7 and cultured for 4 hours. Lycopene and β-carotene were extracted and measured by UHPLC. Error bars are +/- S.D., n=3.

442 **3.5 Coordinated expression of the lycopene and β-carotene BGCs with the dual expression system**

443 Natural products are often encoded by BGCs, and the ability to activate each gene at different
444 time points with different inducers can be advantageous, particularly when the genes are toxic or the
445 metabolites produced by the BGC affect the growth of the heterologous host (Kadjo and Eustáquio 2023).
446 In this study, we have demonstrated that the σ^{70}V2TcR expression system can effectively activate the
447 production of lycopene and β-carotene. As a next step, we attempted to exert control of β-carotene at
448 different points in the production pathway using two different inducers, aTc and IPTG. The LYC operon
449 was integrated into the σ^{70}V2TcR expression system, while the crtY gene was controlled by the σ^{70}V2/3LacI
450 expression system (Fig. 1F). The plasmid pσ^{70}V2TcR-crtEBI/V3LacI-crtY was transformed into *E. coli*, and
451 the plasmid pσ^{70}V2TcR-crtEBI/V2lacI-crtY was transformed into *P. putida* and *V. natriegens*. In all three
452 bacterial species, no lycopene accumulation was observed upon sole induction by aTc despite the crtEBI
453 genes being controlled by the σ^{70}V2TcR expression system (Fig. 4E). This result in *E. coli* can be explained
454 by the leakage of the crtY under the control of the synthetic promoter σ^{70}V3LacI. The high processivity of
455 the lycopene cyclase CrtY to metabolize lycopene directly into β-carotene requires tighter regulation of
456 the promoter to completely repress this gene, and the σ^{70}V3LacI expression systems lacks this control. On
457 the other hand, while the σ^{70}V2TcR-crtEBI system showed no measurable leakage in *P. putida* and *V.*
458 *natriegens* using fluorescent reporters, we previously showed that the σ^{70}V2lacI expression system does
459 leak (Carrillo Rincón and Farny 2023). Consequently, the lycopene produced after the addition of aTc was
460 directly processed into β-carotene by the CrtY present in the cells due to leakage of σ^{70}V2LacI.

461 Production of β-carotene in *E. coli* was observed regardless of the absence or presence of the
462 inducers aTc and IPTG (Fig. 4F), demonstrating that the dual σ^{70}V2TcR/ σ^{70}V3LacI expression system would
463 require tighter regulation in the OFF state to effectively downregulate the target gene in the absence of
464 the inducer. In *P. putida* and *V. natriegens*, production of β-carotene was only achieved when the cultures
465 were induced with aTc or with aTc+IPTG (Fig. 4F). IPTG induction alone did not lead to β-carotene

466 production because the crtEBI genes were not transcribed by the σ^{70}V2TcR expression system. Addition
467 of aTc resulted in β-carotene levels similar to the ones obtained when the cells were induced with
468 aTc+IPTG (Fig. 4F), thus indicating that the minimal leakage of the σ^{70}V2lacI-crtY in *P. putida* and *V.*
469 *natriegens* is sufficient to metabolize all lycopene produced by the σ^{70}V2TcR-crtEBI immediately into β-
470 carotene upon induction by aTc. The varying yields of β-carotene between *E. coli*, *P. putida*, and *V.*
471 *natriegens* highlight the differences in their suitability as hosts for natural product production. While *E.*
472 *coli* may struggle to efficiently produce complex products from BGCs, *P. putida* and *V. natriegens* appear
473 to be well-suited for this task, as evidenced by their superior performance in this study, almost doubling
474 the yields obtained from *E. coli*.

475

476 **3.6 Adaptation of toehold switch to the synthetic σ^{70} expression systems and fold-change evaluation**
477 **with the reporter system mCardinal**

478 The assessment of σ^{70} expression systems using the reporter mCardinal suggested that the
479 σ^{70}V2TcR promoter displays tight regulation, leading to undetectable levels of red fluorescence in the
480 uninduced state (Carrillo Rincón and Farny 2023). However, when the LYC operon and crtY were
481 incorporated into this synthetic promoter, lycopene and β-carotene were produced by *E. coli* in the
482 uninduced state, indicating that the promoter was not completely repressed. The processivity of enzymes,
483 unlike static fluorescent proteins, amplifies the effect of leaky transcription. In the σ^{70}V2/3LacI expression
484 systems the leakage was even more evident, as we were unable to repress the production of CrtY in the
485 dual expression system sufficiently to permit the intermediate accumulation of lycopene (Fig. 4E, F).
486 Maintaining low basal expression levels in the absence of the inducer is crucial to minimize unwanted
487 effects on cell growth and to prevent potential damage caused by the target protein, including issues like
488 self-aggregation or inclusion body formation (Schuster and Reisch 2022), or as evidenced in this study,

489 uncontrolled biosynthesis of a downstream product. If independent control of steps within a multistep
490 biosynthetic pathway is to be achieved, it will require significant improvements in control of inducible
491 promoter systems.

492 One solution to this problem involves the adaptation of RNA-based gene regulation to the gene
493 circuits to reducing the impact of basal expression (Hwang, Kim et al. 2021, Wang and Simmel 2022). The
494 current design of the synthetic σ^{70} expression system comprises a transcriptional control performed by
495 the transcriptional regulators TetR and LacI. Introducing an additional translational control mechanism,
496 such as a toehold switch (THS), alongside the existing transcriptional control, could enhance the precision
497 of the σ^{70} expression systems. This added layer of regulation could provide finer control over gene
498 expression, potentially reducing leakiness and improving inducibility. To this end, the σ^{70}V2TcR and
499 σ^{70}V2lacI expression systems were modified with the incorporation of the three components required to
500 add toehold-mediated translational control: the THS trigger, the THS target and the RBS (Green, Silver et
501 al. 2014). For the σ^{70}V2TcR expression system, two σ^{70}V2Tc promoters were incorporated into the system,
502 the first σ^{70}V2Tc promoter regulates the transcription of the THS trigger, while the second promoter is
503 fused to the THS target, which masks the RBS (Fig. 5A). The σ^{70}V2lacI follows the same architecture, except
504 the THS trigger is regulated by the V3Lac promoter due its reduced leakage compared to the V2Lac, which
505 controls the THS target that hides the RBS (Fig. 5B). This arrangement combines transcriptional and
506 translation regulation, therefore, the absence of the inducers (aTc or IPTG) results in both transcriptional
507 repression (via the transcriptional regulators TetR and LacI) and translational repression (via the THS
508 trigger) of mCardinal. Upon addition of the inducers, the constitutively expressed transcriptional
509 regulators are removed from the synthetic σ^{70} promoters, activating the transcription of the THS trigger,
510 which binds to the THS target inducing the conformational change that relieves the translational
511 repression of mCardinal resulting in its subsequent expression.

512 The comparison between the uninduced and induced states of the σ^{70}V2TcR expression system
513 with and without the toehold switch revealed very similar induction dynamics, as expected (Fig. 5C). It
514 was previously determined that the leakiness of σ^{70}V2TcR could not be observed with a fluorescent
515 reporter. The system may exhibit leakage even with the addition of the THS, but it would not be detectable
516 in this assay. The addition of aTc facilitated mCardinal production by both promoters. However, the
517 promoter with the THS exhibited a 2-fold reduction in the dynamic range compared to the promoter
518 without the switch, although it still maintained a satisfactory level of recombinant protein production (Fig.
519 5D). On the other hand, the addition of the THS had a significant effect on suppressing leaky transcription
520 from the σ^{70}V2lacI expression system (Fig. 5E). The dynamic range in the THS-σ^{70}V2lacI system improved
521 by 5.7-fold, but still, leaky transcription was significant. However, the riboswitch did reduce the leakiness
522 by 7-fold compared to the original version (Fig. 5F). Importantly, mCardinal production after IPTG
523 induction reached similar levels in both σ^{70}V2lacI expressions, with the variant lacking the THS producing
524 1.2-fold more mCardinal (Fig. 5).

525 These results demonstrate that THSs enhance the regulation of gene expression by modulating
526 translation initiation. This feature is particularly effective in inducible expression systems prone to
527 leakage. However, while fluorescent proteins like mCardinal offer valuable insights, they might not
528 capture the subtle nature of basal transcription. For instance, the evaluation of the σ^{70}V2TcR expression
529 system using fluorescent proteins indicated complete lack of fluorescent protein synthesis in the OFF state
530 when uninduced. However, the results presented for the production of lycopene in the dual expression
531 system revealed that the promoter leaks to some extent. Therefore, to truly assess any basal
532 transcriptional activity, the use of enzymatic reporter systems will be necessary, with higher sensitivity
533 for accurately evaluating gene expression dynamics.

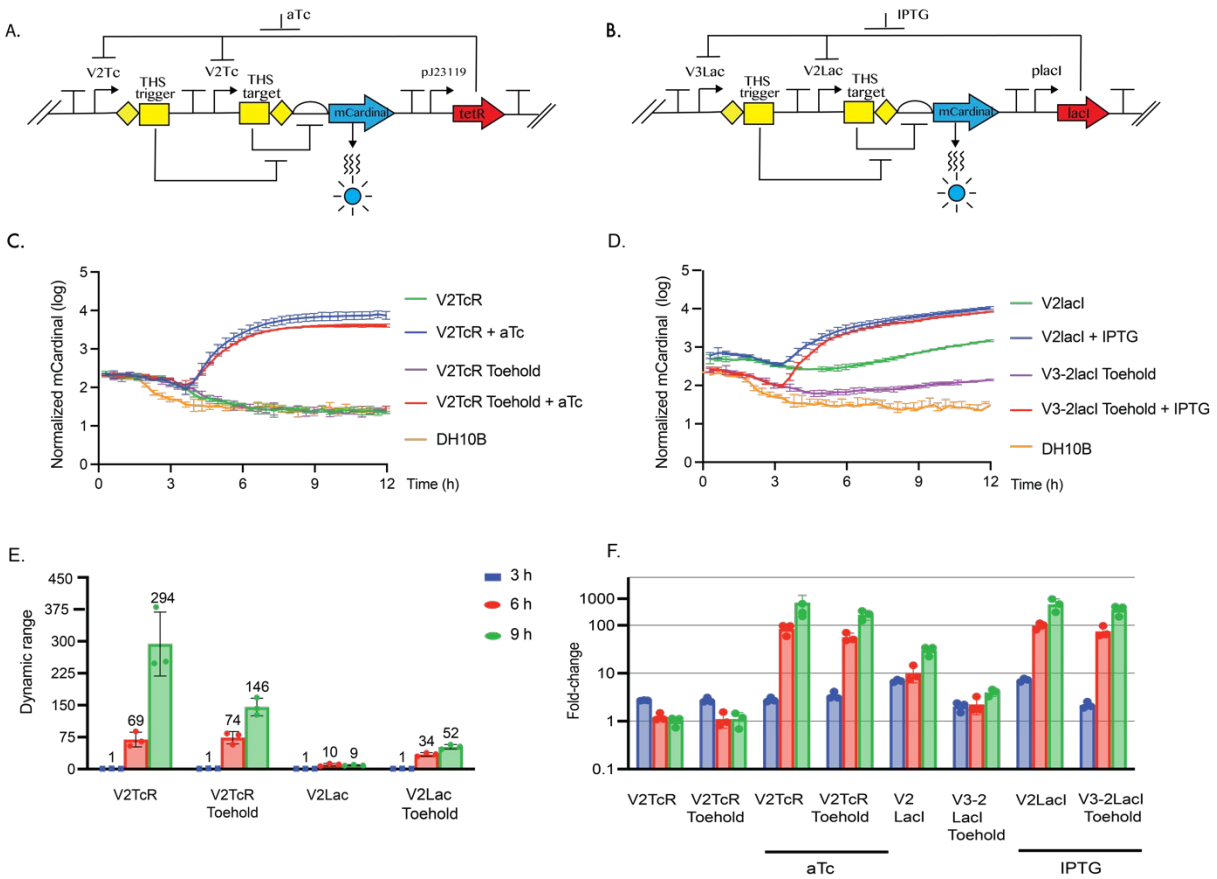

Figure 5. Comparison of the σ^{70} expression systems to the toehold versions controlling the expression of the reporter system mCardinal in *E. coli*. A-B. Architecture of the synthetic gene circuits with the toehold switches (THSs) in the σ^{70}V2TcR system (A), and in the σ^{70}V3-2LacI system (B). **C**. Time course of mCardinal production by pσ^{70}V2TcR-Toehold. **D**. Time course of mCardinal production by σ^{70}V3-2LacI. **E.** Difference in mCardinal production between the ON and OFF states. **F**. Fold-change difference in the red-light emission of the recombinant cells vs the wild type DH10B. The cultures were induced after 3 hours of growth with aTc or IPTG accordingly. For all samples, the fluorescence mean of mCardinal signal (excitation 605, emission 659) was normalized by the cell density (OD_{600}). Error bars are +/- S.D., n=3.

3.7 Evaluation of the *σ^{70}* expression systems using luciferase as a reporter

The selection of the red fluorescent protein mCardinal to estimate the efficiency of the *σ^{70}* expression systems was a strategic choice, to circumvent intrinsic issues associated with sfGFP and the potential interference of green autofluorescence from cells, which could lead to inaccurate quantification of the recombinant protein produced by the synthetic promoters (Carrillo Rincón and Farny 2023). However, upon assessing the synthetic promoters for terpenoid production, it became evident that the *σ^{70}*V2TcR expression system does display leaky transcription, a phenomenon not discernible with mCardinal as the reporter. The integration of the THS into *σ^{70}*V2lacI effectively mitigated basal expression.

550 However, this effect was not evident in THS-σ^{70}V2TcR-mCardinal, as undetectable fluorescence in the OFF
551 state in this expression system was achieved even without the THS. The terpenoids lycopene and β-
552 carotene, aside from their nutraceutical properties, can serve as reporter systems due to their ability to
553 induce a color change in the cell biomass upon production (McNerney and Styczynski 2017). Indeed, the
554 biosynthesis of these pigments was instrumental in detecting the leakage of the σ^{70}V2TcR system.
555 However, accurate estimation of terpenoid yields necessitates laborious compound isolation techniques
556 and complex measurements. Consequently, their use as a reporter system may not be the ideal choice for
557 evaluating the metrics of an inducible system. To comprehensively grasp the behavior of the synthetic σ^{70}
558 expression systems and address the challenges posed by the limited sensitivity of mCardinal and the
559 intricate evaluation of terpenoid production, we opted to employ luciferase as a reporter.

560 The bacterial luciferase, encoded by the lux operon (luxCDABE), initiates the emission of
561 bioluminescence upon its expression, without requiring the addition of an external substrate (Hakkila,
562 Maksimow et al. 2002). The luciferase reporter was integrated into the σ^{70} expression systems and their
563 corresponding THS variants (Fig. 6A, B) to amplify the detection of basal expression levels, particularly in
564 the σ^{70}V2TcR system where the uninduced state appears completely OFF when using mCardinal (Carrillo
565 Rincón and Farny 2023), yet shows activity with lycopene and β-carotene. The time course evaluation
566 permitted the visualization of the leakage of the σ^{70}V2TcR, and also confirmed that the THS version of this
567 promoter diminished the leakage and amplified the signal of bioluminescence (Fig. 6C, E, G). Interestingly,
568 bioluminescence production with the riboswitch tends to diminish over time, suggesting that translational
569 regulation favors the repression of the lux operon after the mid-log phase of growth. In contrast, the
570 original σ^{70}V2TcR system maintains its pronounced leakage over time (Fig. 6G). In the σ^{70}V2lacI expression
571 system, the THS version exhibited a similar pattern to the THS- σ^{70}V2TcR system in both induced and
572 uninduced states, with higher basal levels, as expected (Fig 6H). The σ^{70}V2lacI variant, on the other hand,
573 exhibited higher leakage (Fig. 6D). Interestingly, induction with IPTG halted bioluminescence production

574 (Fig. 6D). This phenomenon may be attributed to the potency of this promoter, whose activation could
575 exceed the metabolic capacity of the cells. These results demonstrate that the reporter luciferase provides
576 a more sensitive assessment of the expression levels in the uninduced state compared to fluorescent
577 proteins like mCardinal. Importantly, the translational regulation provided by the toehold switches
578 efficiently amplifies the fold change and reduces the basal expression levels of the σ^{70} expression systems,
579 thereby improving the tight regulation of the promoters while maintaining their strength (Fig 6E, F).
580 However, total repression was not achieved by the adaptation of the toehold riboregulator as the
581 σ^{70}V2TcR-toehold expression system showed minimal (Fig 6G), and the σ^{70}V3-2LacI pronounced (Fig. 6H)
582 leakiness, thus prohibiting total control of the target recombinant genes.

583 Total gene expression control is crucial for regulating enzymatic reactions involved in the
584 biosynthesis of natural products, as demonstrated with the production of terpenes presented in this
585 study. The synthetic expression systems evaluated in this study were evaluated in the pJH0204 plasmid
586 which contains the pColE1 origin of replication (Carrillo Rincón and Farny 2023). This plasmid has the
587 advantage to integrate in the chromosome of *P. putida* and replicate in *V. natriegens*, therefore offers a
588 platform to use multiple chassis (Carrillo Rincón and Farny 2023). However, one potential disadvantage
589 of this plasmid in *E. coli* is the copy number. The pColE1 origin of replication produces 25–30 copies per
590 cell in *E. coli* (Hershfield, Boyer et al. 1974). To achieve tighter control over gene expression, we
591 transferred the synthetic expression systems to the low copy plasmid pSC101, which has approximately 3
592 copies per cell (Joshi, Yong et al. 2022). In this configuration, both σ^{70}V2TcR expression systems achieved
593 total repression of the lux operon in the uninduced state, thus indicating that in the σ^{70}V2TcR expression
594 system the transcriptional control provided by TetR is enough to shut down the σ^{70}V2Tc promoter (Fig.
595 6C, E, G). Activation by aTc successfully induced bioluminescence production; however, the THS-version
596 produced ∼2-fold less light, indicating that the translational control provided by the toehold affects the
597 activity of the promoter (Fig. 6C, E, G). A similar trend was observed with the σ^{70}V2LacI and σ^{70}V3-2LacI

598 expression systems in pSC101 (Fig 6D, F, H). Although total repression was not achieved, the translational
599 control provided by the toehold significantly reduced the basal expression levels and amplified the
600 dynamic range of the strong σ^{70}V2Lac promoter (Fig. 6E, H), the strongest promoter within the family of
601 σ^{70} expression systems.

602 In *P. putida*, the pJH0204 plasmid integrates at one specific location in the chromosome (Elmore,
603 Furches et al. 2017). In this configuration, using mCardinal as the reporter system, the σ^{70}V2TcR showed
604 no leakage, while the σ^{70}V2LacI exhibited minimal, barely detectable red fluorescence in the uninduced
605 state (Carrillo Rincón and Farny 2023). However, traces of lycopene and β-carotene were detected in the
606 uninduced state of the σ^{70}V2TcR (Fig. 4A, B), and only β-carotene was produced in the dual system (Fig.
607 4C &D), thus corroborating the leakage of σ^{70}V2LacI in this host. Since the transcriptional control provided
608 by the regulatory proteins TetR and/or LacI proved insufficient to fully repress the σ^{70} synthetic promoters,
609 even at one copy per cell, we decided to incorporate translation repression in *P. putida*. The luciferase
610 reporter system confirmed the leakage of the σ^{70} expression systems in this host (Fig. 7D), and the addition
611 of the toehold amplified the dynamic range and reduced the luminescence emission in the uninduced by
612 ~2-fold in both expression systems (Fig. 7D). These results demonstrate that the transcriptional control
613 provided by the regulatory proteins can be enhanced by translational control via THS in *P. putida*, as noted
614 in the σ^{70}V2TcR system. However, these two layers of control are not sufficient to completely turn off the
615 σ^{70}V2LacI expression system. Unlike in *E. coli*, plasmid copy number is not a parameter that could be
616 further optimized in *P. putida. V. natriegens*, on the other hand, has demonstrated the ability to maintain
617 different plasmids with various origins of replication, including pUC, pSC101, p15a, and pBR1 (Tschirhart,
618 Shukla et al. 2019). The pJH0204, derivative of pColE1 ori, shows the highest copy number in this host
619 with 313 copies per cell (Tschirhart, Shukla et al. 2019). Therefore, we speculate that using a low-copy
620 plasmid in conjunction with the THS could also improve the control of the synthetic σ^{70} expression system
621 in this chassis bacteria.

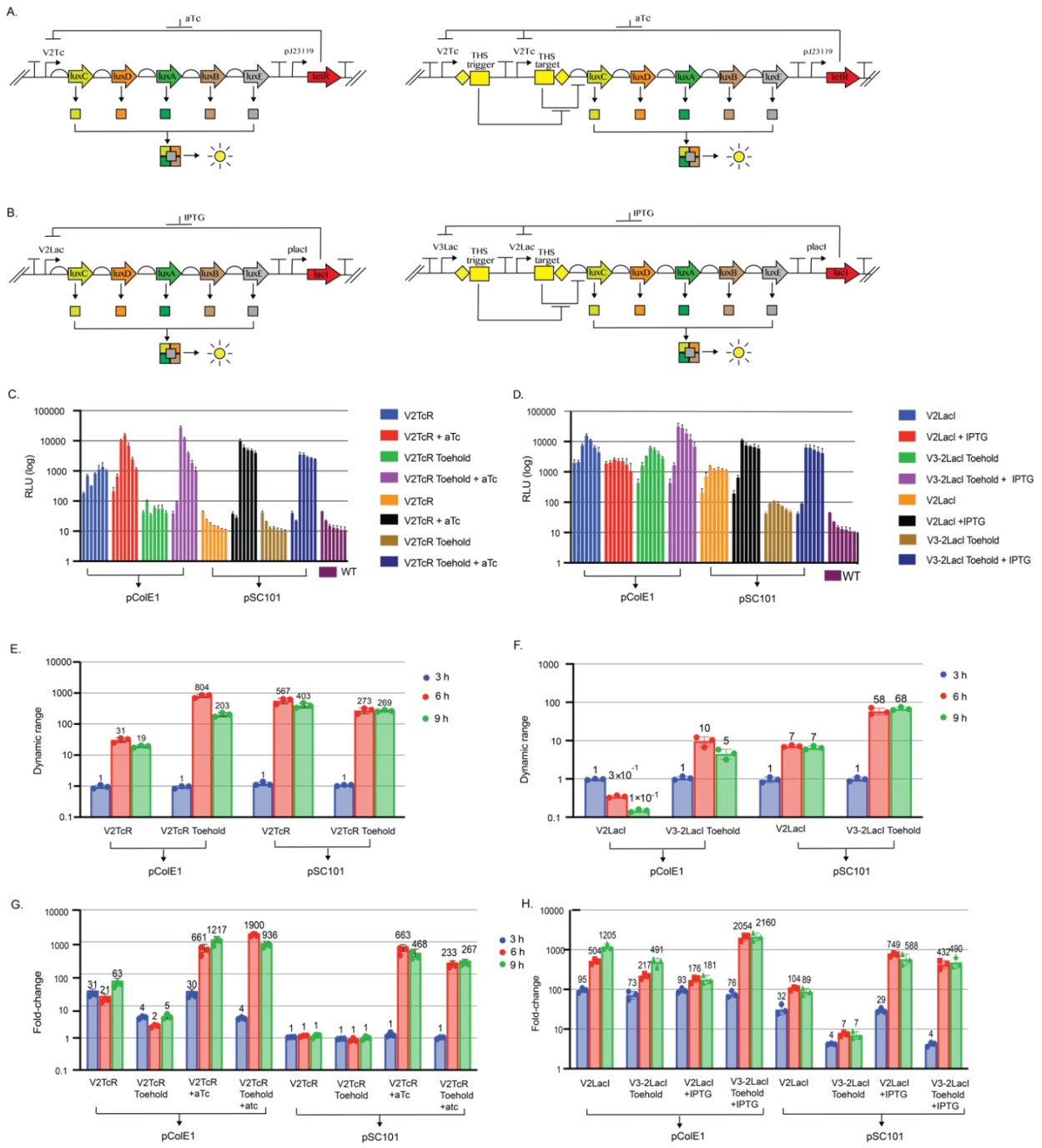

Figure 6. Comparison of the σ^{70} expression systems to the toehold versions controlling the expression of the lux operon in *E. coli* using pCOLE1 and pSC101 derived plasmids. **A-B**. Architecture of the synthetic gene circuits controlling the luxCDABE genes with and without the THS in σ^{70}V2TcR system (A), and in σ^{70}V3-2LacI system (B). **C-D**. Time course of bioluminescence production by the pσ^{70}V2TcR (C) and pσ^{70}V3-2LacI (D) expression systems; each bar represents the bioluminescence measurement after 3 hours of growth from time 0 to 18 hours. **E-F.** Difference in bioluminescence production between the ON and OFF states in pσ^{70}V2TcR (E) and pσ^{70}V3-2LacI (F) expression systems. **G-H**. Fold-change difference in the light emission of the recombinant cells containing the pσ^{70}V2TcR (G) and pσ^{70}V3-2LacI (H) expression systems vs the wild type DH10B. The cultures were induced after 3 hours of growth with aTc or IPTG accordingly. For all samples, the bioluminescence mean was normalized by the cell density (OD_{600}). Error bars are +/- S.D., n=3.

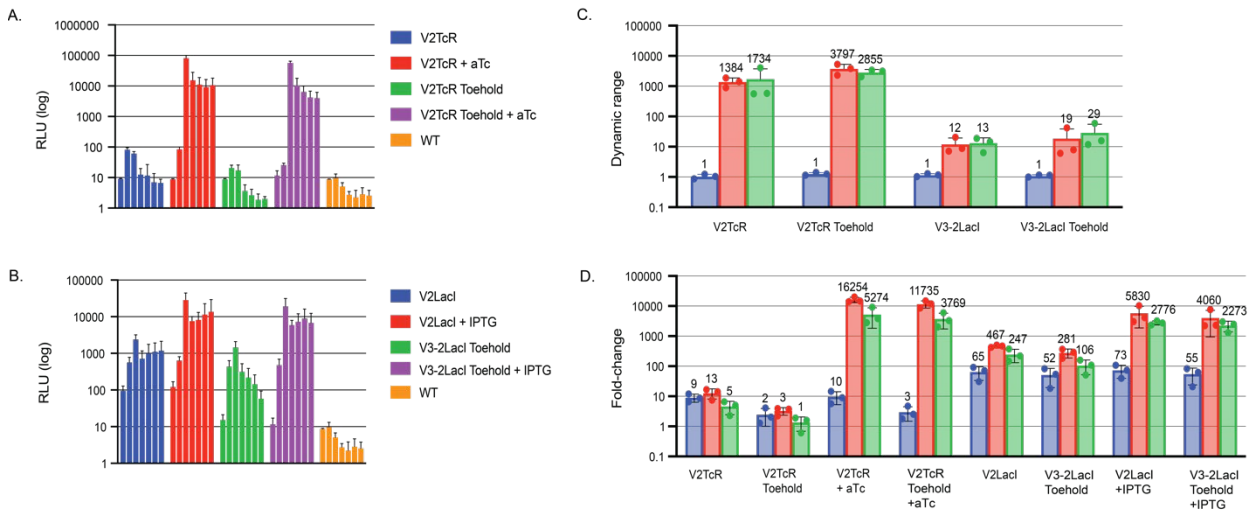

Figure 7. Comparison of the σ^{70} expression systems to the toehold versions controlling the expression of the lux operon in *P. putida*. A-B. Time course of bioluminescence production by the pσ^{70}V2TcR (A) and pσ^{70}V3-2LacI (B) expression systems; each bar represents the bioluminescence measurement after 3 hours of growth from time 0 to 18 hours. **C.** Difference in bioluminescence production between the ON and OFF states in pσ^{70}V2TcR and pσ^{70}V3-2LacI expression systems. **D**. Fold-change difference in the light emission of the recombinant cells containing the pσ^{70}V2TcR or and pσ^{70}V3-2LacI expression systems vs the wild type *P. putida*. The cultures were induced after 3 hours of growth with aTc or IPTG accordingly. For all samples, the bioluminescence mean was normalized by the cell density (OD_{600}). Error bars are +/- S.D., n=3.

Conclusions

The development of various bacterial chassis has garnered attention in pursuit of the goals of next-generation industrial biotechnology (NGIB) (Yu, Wu et al. 2019). NGIB aims to utilize low-cost mixed substrates, minimize freshwater consumption, save energy, and implement long-lasting, continuous, intelligent processing methods (Yu, Wu et al. 2019). Despite the numerous advantages of *E. coli*, such as its robust genetic toolbox and standardized cultivation parameters (Kent and Dixon 2020, Ruiz and Silhavy 2022), it falls short of achieving the goals of NGIB due to its sensitivity to harsh environments and limited metabolic capabilities (De Wannemaeker, Bervoets et al. 2022, Zhang, Ottenheim et al. 2022). Alternative hosts may be more attractive to accomplish complex tasks. For example, *P. putida* metabolic versatility has a demonstrated ability to utilize lignin-derived compounds, sustain difficult redox reactions, tolerance

652 to organic solvents and stresses associated with industrial-scale cultivations, and shows a relatively high
653 GC-content similar to that of actinomycete-derived natural product BGCs (Nikel and de Lorenzo 2018,
654 Cook, Jacobson et al. 2021, Martin-Pascual, Batianis et al. 2021). The marine bacterium *V. natriegens*,
655 inherently halophilic, offers interesting advantages as well, such as rapid growth and a versatile
656 metabolism capable of utilizing a variety of substrates as carbon and energy sources (Hoff, Daniel et al.
657 2020, Thiele, Gutschmann et al. 2021, Thoma and Blombach 2021). Other non-model Gram-negative
658 bacterial chassis also demonstrate the potential to outperform *E. coli* (Calero and Nikel 2019, Ye and Chen
659 2021). However, each chassis necessitates the adaptation of distinct genetic tools. The σ^{70} expression
660 system showcased in this study, whether used individually or in combination, offers a promising solution
661 to the ongoing challenge of developing numerous host organisms. It provides a versatile and robust gene
662 expression platform with a broad host range. Consequently, proteins or BGCs of interest can be readily
663 cloned into each σ^{70} expression system and evaluated across various chassis, thereby expediting the
664 optimization process.

665 In this study, we selected chassis bacteria commonly used by the scientific community and,
666 through the straightforward incorporation of synthetic gene pathways for the biosynthesis of lycopene
667 and β-carotene, achieved high titers of these terpenoids using the σ^{70} expression system. Notably, no
668 media optimization was necessary to complete this task, highlighting a remarkable advantage offered by
669 the σ^{70} expression system. However, the production of terpenoids using the first generation of the σ^{70}
670 expression system revealed leakage in the OFF state, a feature imperceptible when using fluorescent
671 proteins as a reporter system. Approaches like decreasing plasmid copy number, weakening the RBS
672 sequences, and introducing mutations in the consensus promoter sequences have demonstrated the
673 ability to minimize leakage in the basal state, albeit at the cost of reducing the induced expression levels
674 (Calles, Goñi-Moreno et al. 2019). The strength and portability of the σ^{70} expression systems reside in the
675 specific nucleotide arrangement of the promoter and RBS DNA sequence (Carrillo Rincón and Farny 2023);

676 therefore, altering these sequences was not an option. Instead, the adaptation of the riboswitch toehold,
677 together with the use of a low-copy plasmid in *E. coli*, reduced the leakage of the σ^{70}V2TcR THS to non-
678 detectable levels and nearly abolished the basal expression levels of the σ^{70}V3-2LacI. This approach not
679 only amplified the dynamic range but also maintained the portability of the synthetic expression systems.
680 This was demonstrated in *P. putida*, where the DNA was integrated into the chromosome, and both THS
681 σ^{70} expression systems maintained strong induction, with the σ^{70}V2TcR THS reaching virtually zero
682 transcription. The second generation of the σ^{70} expression system (with THS) remains digital, with ON and
683 OFF state only, however, the emergence of plasmid like TULIP (TUnable Ligand Inducible Plasmid) with
684 controllable copy number (Joshi, Yong et al. 2022) could allow an analogue behavior of the versatile σ^{70}
685 expression systems.

686 In conclusion, the expression system developed in this study expands the genetic toolkit of various
687 promising Gram-negative chassis, thereby enhancing their capabilities to address fundamental biological
688 questions and bolster their biotechnological applications. Ultimately, the σ^{70} expression system has the
689 potential to facilitate the expression of biosynthetic gene clusters (BGCs) that have previously been
690 inaccessible or suboptimal due to the lack of appropriate gene tools or the limitations of model organisms
691 such as *E. coli*.

692

693 **Declarations**

694 **Ethics approval and consent to participate:** Not applicable.

695 **Consent for publication:** Not applicable.

696 **Availability of data and materials:** The raw datasets used and/or analyzed during the current study are
697 available from the corresponding author at reasonable request. All processed data generated or
698 analyzed during this study are included in this published article and its supplementary information files.

699 **Competing interests:** A.F.C.R and N.G.F have filed a U.S. patent application for the pσ^{70} *lac* and *tet*
700 promoters described in this work.

701 **Funding:** This work was supported by new faculty start-up funds from Worcester Polytechnic Institute to
702 N.G.F. & the Sandooq Al Watan grant PRJ-SWARD-256 to A.G.

703 **Authors' contributions**

704 **Andres Felipe Carrillo Rincón:** Conceptualization (lead); data curation (lead); formal analysis (lead);
705 investigation (lead); methodology (lead); resources (equal); validation (lead); visualization (lead); writing
706 – original draft (lead); writing – review and editing (equal).

707 **Alexandra J. Cabral**: Investigation (supporting); methodology (supporting); validation (supporting);
708 visualization (supporting); writing – review and editing (supporting).

709 **Andras Gyorgy** Conceptualization (supporting); funding acquisition (lead); project administration (lead);
710 resources (lead); supervision (supporting); writing – original draft (supporting); writing – review and
711 editing (supporting).

712 **Natalie Gilks Farny:** Conceptualization (supporting); funding acquisition (lead); project administration
713 (lead); resources (lead); supervision (lead); writing – original draft (equal); writing – review and editing
714 (equal).

715

716 **Acknowledgements:** We thank Adam Guss of Oak Ridge National Laboratory for *P. putida* strains and
717 plasmids; Kevin Keating, Emma Tobin, and Eric Young of WPI for assistance with UHPLC experiments and
718 for the gift of crtEBIY genes; Shimshon Belkin of Hebrew University of Jerusalem for the luxCDABE
719 operon.

720

721

722

723 **References**

724 Alper, H., K. Miyaoku and G. Stephanopoulos (2005). "Construction of lycopene-overproducing E. coli
725 strains by combining systematic and combinatorial gene knockout targets." Nat Biotechnol **23**(5): 612-
726 616.

727 Baeshen, M. N., A. M. Al-Hejin, R. S. Bora, M. M. Ahmed, H. A. Ramadan, K. S. Saini, N. A. Baeshen and E.
728 M. Redwan (2015). "Production of Biopharmaceuticals in E. coli: Current Scenario and Future
729 Perspectives." J Microbiol Biotechnol **25**(7): 953-962.

730 Becker, W., F. Wimberger and K. Zangger (2019). "Vibrio natriegens: An Alternative Expression System
731 for the High-Yield Production of Isotopically Labeled Proteins." Biochemistry **58**(25): 2799-2803.

732 Bie, L., M. Zhang, J. Wang, M. Fang, L. Li, H. Xu and M. Wang (2023). "Comparative Analysis of
733 Transcriptomic Response of Escherichia coli K-12 MG1655 to Nine Representative Classes of Antibiotics."
734 Microbiol Spectr **11**(2): e0031723.

735 Bohoyo-Gil, D., D. Dominguez-Valhondo, J. J. García-Parra and D. González-Gómez (2012). "UHPLC as a
736 suitable methodology for the analysis of carotenoids in food matrix." European Food Research and
737 Technology **235**(6): 1055-1061.

738 Calero, P. and P. I. Nikel (2019). "Chasing bacterial chassis for metabolic engineering: a perspective
739 review from classical to non-traditional microorganisms." Microb Biotechnol **12**(1): 98-124.

740 Calles, B., Á. Goñi-Moreno and V. de Lorenzo (2019). "Digitalizing heterologous gene expression in
741 Gram-negative bacteria with a portable ON/OFF module." Mol Syst Biol **15**(12): e8777.

742 Canty, L., S. Hariharan, Q. Liu, S. A. Haney and D. W. Andrews (2018). "Peak emission wavelength and
743 fluorescence lifetime are coupled in far-red, GFP-like fluorescent proteins." PLoS One **13**(11): e0208075.

744 Carrillo Rincón, A. F. and N. G. Farny (2023). "Unlocking the strength of inducible promoters in Gram-
745 negative bacteria." Microb Biotechnol.

746 Cook, T. B., T. B. Jacobson, M. V. Venkataraman, H. Hofstetter, D. Amador-Noguez, M. G. Thomas and B.
747 F. Pfleger (2021). "Stepwise genetic engineering of Pseudomonas putida enables robust heterologous
748 production of prodigiosin and glidobactin A." Metab Eng **67**: 112-124.

749 De Wannemaeker, L., I. Bervoets and M. De Mey (2022). "Unlocking the bacterial domain for industrial
750 biotechnology applications using universal parts and tools." Biotechnol Adv **60**: 108028.

751 Ellis, G. A., T. Tschirhart, J. Spangler, S. A. Walper, I. L. Medintz and G. J. Vora (2019). "Exploiting the
752 Feedstock Flexibility of the Emergent Synthetic Biology Chassis Vibrio natriegens for Engineered Natural
753 Product Production." Mar Drugs **17**(12).

754 Elmore, J. R., G. N. Dexter, H. Baldino, J. D. Huenemann, R. Francis, G. L. t. Peabody, J. Martinez-Baird, L.
755 A. Riley, T. Simmons, D. Coleman-Derr, A. M. Guss and R. G. Egbert (2023). "High-throughput genetic
756 engineering of nonmodel and undomesticated bacteria via iterative site-specific genome integration."
757 Sci Adv **9**(10): eade1285.

758 Elmore, J. R., A. Furches, G. N. Wolff, K. Gorday and A. M. Guss (2017). "Development of a high efficiency
759 integration system and promoter library for rapid modification of Pseudomonas putida KT2440." Metab
760 Eng Commun **5**: 1-8.

761 Gauttam, R., C. Desiderato, L. Jung, A. Shah and B. J. Eikmanns (2019). "A step forward: Compatible and
762 dual-inducible expression vectors for gene co-expression in Corynebacterium glutamicum." Plasmid **101**:
763 20-27.

764 Gauttam, R., A. Mukhopadhyay, B. A. Simmons and S. W. Singer (2021). "Development of dual-inducible
765 duet-expression vectors for tunable gene expression control and CRISPR interference-based gene
766 repression in Pseudomonas putida KT2440." Microb Biotechnol **14**(6): 2659-2678.

767 Gauttam, R., A. Mukhopadhyay and S. W. Singer (2020). "Construction of a novel dual-inducible duet-
768 expression system for gene (over)expression in Pseudomonas putida." Plasmid **110**: 102514.

769 Gemperlein, K., M. Hoffmann, L. Huo, P. Pilak, L. Petzke, R. Müller and S. C. Wenzel (2017). "Synthetic
770 biology approaches to establish a heterologous production system for coronatines." Metab Eng **44**: 213-
771 222.

772 Gemperlein, K., G. Zipf, H. S. Bernauer, R. Müller and S. C. Wenzel (2016). "Metabolic engineering of
773 Pseudomonas putida for production of docosahexaenoic acid based on a myxobacterial PUFA synthase."
774 Metab Eng **33**: 98-108.

775 Gomez-Escribano, J. P., S. Alt and M. J. Bibb (2016). "Next Generation Sequencing of Actinobacteria for
776 the Discovery of Novel Natural Products." Mar Drugs **14**(4).

777 Gong, T., R. Liu, Y. Che, X. Xu, F. Zhao, H. Yu, C. Song, Y. Liu and C. Yang (2016). "Engineering
778 Pseudomonas putida KT2440 for simultaneous degradation of carbofuran and chlorpyrifos." Microb
779 Biotechnol **9**(6): 792-800.

780 Green, A. A., P. A. Silver, J. J. Collins and P. Yin (2014). "Toehold switches: de-novo-designed regulators
781 of gene expression." Cell **159**(4): 925-939.

782 Gyorgy, A., J. I. Jiménez, J. Yazbek, H. H. Huang, H. Chung, R. Weiss and D. Del Vecchio (2015). "Isocost
783 Lines Describe the Cellular Economy of Genetic Circuits." Biophys J **109**(3): 639-646.

784 Hakkila, K., M. Maksimow, M. Karp and M. Virta (2002). "Reporter genes lucFF, luxCDABE, gfp, and dsred
785 have different characteristics in whole-cell bacterial sensors." Anal Biochem **301**(2): 235-242.

786 Hernandez-Arranz, S., J. Perez-Gil, D. Marshall-Sabey and M. Rodriguez-Concepcion (2019). "Engineering
787 Pseudomonas putida for isoprenoid production by manipulating endogenous and shunt pathways
788 supplying precursors." Microb Cell Fact **18**(1): 152.

789 Hershfield, V., H. W. Boyer, C. Yanofsky, M. A. Lovett and D. R. Helinski (1974). "Plasmid ColEl as a
790 molecular vehicle for cloning and amplification of DNA." Proc Natl Acad Sci U S A **71**(9): 3455-3459.

791 Hoff, J., B. Daniel, D. Stukenberg, B. W. Thuronyi, T. Waldminghaus and G. Fritz (2020). "Vibrio
792 natriegens: an ultrafast-growing marine bacterium as emerging synthetic biology chassis." Environ
793 Microbiol **22**(10): 4394-4408.

794 Hwang, Y., S. G. Kim, S. Jang, J. Kim and G. Y. Jung (2021). "Signal amplification and optimization of
795 riboswitch-based hybrid inputs by modular and titratable toehold switches." J Biol Eng **15**(1): 11.

796 İncir, İ. and Ö. Kaplan (2024). "Escherichia coli as a versatile cell factory: Advances and challenges in
797 recombinant protein production." Protein Expr Purif **219**: 106463.

798 Jensen, P. R. (2016). "Natural Products and the Gene Cluster Revolution." Trends Microbiol **24**(12): 968-
799 977.

800 Joshi, S. H., C. Yong and A. Gyorgy (2022). "Inducible plasmid copy number control for synthetic biology
801 in commonly used E. coli strains." Nat Commun **13**(1): 6691.

802 Kadjo, A. E. and A. S. Eustáquio (2023). "Bacterial natural product discovery by heterologous
803 expression." Journal of Industrial Microbiology and Biotechnology **50**(1).

804 Karnjanawipagul, P., W. Nittayanuntawech, P. Rojsanga and L. Suntornsuk (2010). "Analysis of β-
805 carotene in carrot by spectrophotometry." Mahidol University Journal of Pharmaceutical Science **37**(8).

806 Katz, L. and R. H. Baltz (2016). "Natural product discovery: past, present, and future." J Ind Microbiol
807 Biotechnol **43**(2-3): 155-176.

808 Kelly, C. L., G. M. Taylor, A. Šatkutė, L. Dekker and J. T. Heap (2019). "Transcriptional Terminators Allow
809 Leak-Free Chromosomal Integration of Genetic Constructs in Cyanobacteria." Microorganisms **7**(8).

810 Kent, R. and N. Dixon (2020). "Contemporary Tools for Regulating Gene Expression in Bacteria." Trends
811 Biotechnol **38**(3): 316-333.

812 Krishnamurthi, V. R., Niyonshuti, II, J. Chen and Y. Wang (2021). "A new analysis method for evaluating
813 bacterial growth with microplate readers." PLoS One **16**(1): e0245205.

814 Loeschcke, A. and S. Thies (2015). "Pseudomonas putida-a versatile host for the production of natural
815 products." Appl Microbiol Biotechnol **99**(15): 6197-6214.

816 Lutz, R. and H. Bujard (1997). "Independent and tight regulation of transcriptional units in Escherichia
817 coli via the LacR/O, the TetR/O and AraC/I1-I2 regulatory elements." Nucleic Acids Res **25**(6): 1203-1210.

818 Martin-Pascual, M., C. Batianis, L. Bruinsma, E. Asin-Garcia, L. Garcia-Morales, R. A. Weusthuis, R. van
819 Kranenburg and V. A. P. Martins Dos Santos (2021). "A navigation guide of synthetic biology tools for
820 Pseudomonas putida." Biotechnol Adv **49**: 107732.

821 McNerney, M. P. and M. P. Styczynski (2017). "Precise control of lycopene production to enable a fast-
822 responding, minimal-equipment biosensor." Metab Eng **43**(Pt A): 46-53.

823 Meyer, A. J., T. H. Segall-Shapiro, E. Glassey, J. Zhang and C. A. Voigt (2019). "Escherichia coli
824 "Marionette" strains with 12 highly optimized small-molecule sensors." Nat Chem Biol **15**(2): 196-204.

825 Miguez, A.M., M.P. McNerney, and M. P. Styczynski (2018). "Metabolomics analysis of the toxic effects
826 of the production of lycopene and its precursors." Front Microbiol, **9**, p.324115.

827 Monici, M. (2005). "Cell and tissue autofluorescence research and diagnostic applications." Biotechnol
828 Annu Rev **11**: 227-256.

829 Nakata, P. A. (2017). "Construction of pDUO: A bicistronic shuttle vector series for dual expression of
830 recombinant proteins." Plasmid **89**: 16-21.

831 Nikel, P. I. and V. de Lorenzo (2018). "Pseudomonas putida as a functional chassis for industrial
832 biocatalysis: From native biochemistry to trans-metabolism." Metab Eng **50**: 142-155.

833 Öztürk, S., B. G. Ergün and P. Çalık (2017). "Double promoter expression systems for recombinant
834 protein production by industrial microorganisms." Appl Microbiol Biotechnol **101**(20): 7459-7475.

835 Ringel, M. T. and T. Brüser (2018). "The biosynthesis of pyoverdines." Microb Cell **5**(10): 424-437.

836 Romanuka, J., H. van den Bulke, R. Kaptein, R. Boelens and G. E. Folkers (2009). "Novel strategies to
837 overcome expression problems encountered with toxic proteins: application to the production of Lac
838 repressor proteins for NMR studies." Protein Expr Purif **67**(2): 104-112.

839 Ruiz, N. and T. J. Silhavy (2022). "How Escherichia coli Became the Flagship Bacterium of Molecular
840 Biology." J Bacteriol **204**(9): e0023022.

841 Schuster, L. A. and C. R. Reisch (2022). "Plasmids for Controlled and Tunable High-Level Expression in E.
842 coli." Appl Environ Microbiol **88**(22): e0093922.

843 Snijder, H. J. and J. Hakulinen (2016). "Membrane Protein Production in E. coli for Applications in Drug
844 Discovery." Adv Exp Med Biol **896**: 59-77.

845 Snoeck, S., C. Guidi and M. De Mey (2024). ""Metabolic burden" explained: stress symptoms and its
846 related responses induced by (over)expression of (heterologous) proteins in Escherichia coli." Microb
847 Cell Fact **23**(1): 96.

848 Stetz, M. A., M. V. Carter and A. J. Wand (2016). "Optimized expression and purification of biophysical
849 quantities of Lac repressor and Lac repressor regulatory domain." Protein Expr Purif **123**: 75-82.

850 Thiele, I., B. Gutschmann, L. Aulich, M. Girard, P. Neubauer and S. L. Riedel (2021). "High-cell-density
851 fed-batch cultivations of Vibrio natriegens." Biotechnol Lett **43**(9): 1723-1733.

852 Thoma, F. and B. Blombach (2021). "Metabolic engineering of Vibrio natriegens." Essays Biochem **65**(2):
853 381-392.

854 Tolia, N. H. and L. Joshua-Tor (2006). "Strategies for protein coexpression in Escherichia coli." Nat
855 Methods **3**(1): 55-64.

856 Tschirhart, T., V. Shukla, E. E. Kelly, Z. Schultzhaus, E. NewRingeisen, J. S. Erickson, Z. Wang, W. Garcia, E.
857 Curl, R. G. Egbert, E. Yeung and G. J. Vora (2019). "Synthetic Biology Tools for the Fast-Growing Marine
858 Bacterium Vibrio natriegens." ACS Synth Biol **8**(9): 2069-2079.

859 Wang, H., J. Li and M. C. Jewett (2018). "Development of a Pseudomonas putida cell-free protein
860 synthesis platform for rapid screening of gene regulatory elements." Synth Biol (Oxf) **3**(1): ysy003.

861 Wang, T. and F. C. Simmel (2022). "Riboswitch-inspired toehold riboregulators for gene regulation in
862 Escherichia coli." Nucleic Acids Res **50**(8): 4784-4798.

863 Wang, Z., T. Tschirhart, Z. Schultzhaus, E. E. Kelly, A. Chen, E. Oh, O. Nag, E. R. Glaser, E. Kim, P. F. Lloyd,
864 P. T. Charles, W. Li, D. Leary, J. Compton, D. A. Phillips, A. Dhinojwala, G. F. Payne and G. J. Vora (2020).
865 "Melanin Produced by the Fast-Growing Marine Bacterium Vibrio natriegens through Heterologous
866 Biosynthesis: Characterization and Application." Appl Environ Microbiol **86**(5).

867 Wu, C., Y. Yin, L. Zhu, Y. Zhang and Y. Z. Li (2022). "Metagenomic sequencing-driven multidisciplinary
868 approaches to shed light on the untapped microbial natural products." Drug Discov Today **27**(3): 730-
869 742.

870 Wu, G., Q. Yan, J. A. Jones, Y. J. Tang, S. S. Fong and M. A. G. Koffas (2016). "Metabolic Burden:
871 Cornerstones in Synthetic Biology and Metabolic Engineering Applications." Trends Biotechnol **34**(8):
872 652-664.

873 Xu, J., X. Xu, Q. Xu, Z. Zhang, L. Jiang and H. Huang (2018). "Efficient production of lycopene by
874 engineered E. coli strains harboring different types of plasmids." Bioprocess Biosyst Eng **41**(4): 489-499.

875 Ye, J. W. and G. Q. Chen (2021). "Halomonas as a chassis." Essays Biochem **65**(2): 393-403.

876 Yoon, S. H., H. M. Park, J. E. Kim, S. H. Lee, M. S. Choi, J. Y. Kim, D. K. Oh, J. D. Keasling and S. W. Kim
877 (2007). "Increased beta-carotene production in recombinant Escherichia coli harboring an engineered
878 isoprenoid precursor pathway with mevalonate addition." Biotechnol Prog **23**(3): 599-605.

879 Yu, L. P., F. Q. Wu and G. Q. Chen (2019). "Next-Generation Industrial Biotechnology-Transforming the
880 Current Industrial Biotechnology into Competitive Processes." Biotechnol J **14**(9): e1800437.

881 Zhang, C., L. Liu, L. Teng, J. Chen, J. Liu, J. Li, G. Du and J. Chen (2012). "Metabolic engineering of
882 Escherichia coli BL21 for biosynthesis of heparosan, a bioengineered heparin precursor." Metab Eng
883 **14**(5): 521-527.

884 Zhang, C., C. Ottenheim, M. Weingarten and L. Ji (2022). "Microbial Utilization of Next-Generation
885 Feedstocks for the Biomanufacturing of Value-Added Chemicals and Food Ingredients." Front Bioeng
886 Biotechnol **10**: 874612.

887